

ISTANBUL TECHNICAL UNIVERSITY ★ GRADUATE SCHOOL

**CONTROL OF HOPF AND BAUTIN BIFURCATION
IN A MODIFIED GOODWIN MODEL OF GROWTH CYCLE**



M.Sc. THESIS

Melike Nur ERDOĞAN

Department of Mathematics Engineering

Mathematics Engineering Programme

JUNE 2024

ISTANBUL TECHNICAL UNIVERSITY ★ GRADUATE SCHOOL

**CONTROL OF HOPF AND BAUTIN BIFURCATION
IN A MODIFIED GOODWIN MODEL OF GROWTH CYCLE**

M.Sc. THESIS

**Melike Nur ERDOĞAN
(509201240)**

Department of Mathematics Engineering

Mathematics Engineering Programme

Thesis Advisor: Assoc. Prof. Dr. Ayşe PEKER

JUNE 2024

İSTANBUL TEKNİK ÜNİVERSİTESİ ★ LİSANSÜSTÜ EĞİTİM ENSTİTÜSÜ

**DEĞİŞTİRİLMİŞ GOODWIN BÜYÜME DÖNGÜSÜ MODELİNDE
HOPF VE BAUTIN ÇATALLANMASININ KONTROLÜ**

YÜKSEK LİSANS TEZİ

**Melike Nur ERDOĞAN
(509201240)**

Matematik Mühendisliği Anabilim Dalı

Matematik Mühendisliği Programı

Tez Danışmanı: Assoc. Prof. Dr. Ayşe PEKER

HAZİRAN 2024



FOREWORD

First and foremost, I wish to extend my heartfelt gratitude to my advisor, Assoc. Prof. Dr. Ayşe Peker for her invaluable support and guidance throughout my thesis journey. I would also like to extend my sincere appreciation to Assoc. Prof. Dr. Cihangir Özemir who provided invaluable guidance and support throughout my thesis process. Their unwavering commitment and mentorship have been instrumental in shaping my academic growth and success. Their expertise, encouragement, and willingness to invest time and effort in my development have fostered a profoundly enriching and productive study experience. Working alongside them has been a privilege, and I am deeply grateful for the opportunity to learn from their wisdom and expertise.

Furthermore, I am profoundly appreciative of my cherished family—my parents and siblings—for their unwavering encouragement, understanding, and sacrifices they have made to support my educational pursuits. Their unwavering belief in me and their continuous motivation have been a constant source of strength and inspiration throughout this journey.

June 2024

Melike Nur ERDOĞAN



TABLE OF CONTENTS

	<u>Page</u>
FOREWORD	vii
TABLE OF CONTENTS	ix
ABBREVIATIONS	xi
SYMBOLS	xiii
LIST OF TABLES	xv
LIST OF FIGURES	xvii
SUMMARY	xix
ÖZET	xxiii
1. INTRODUCTION	1
1.1 Purpose of Thesis	1
1.2 Literature Review	1
1.3 Hypothesis & Research Questions	3
2. NONLINEAR DYNAMICAL SYSTEMS, STABILITY AND CONTROL	5
2.1 Bifurcation Theory and Stability	6
2.1.1 Hopf bifurcation.....	8
2.1.2 Bautin bifurcation	16
2.2 Control of Hopf and Bautin Bifurcation.....	20
2.3 Goodwin Model and Modifications.....	21
2.3.1 Original Goodwin model	21
2.3.2 Desai's modified Goodwin model.....	22
3. CONTROL OF HOPF AND BAUTIN BIFURCATION IN A MODIFIED GOODWIN MODEL	23
3.1 Equilibrium and Linearisation.....	23
3.2 Control of Hopf Bifurcation	25
3.3 Control of Bautin Bifurcation.....	30
4. CONCLUSIONS AND RECOMMENDATIONS	39
4.1 Conclusions	39
4.2 Future Suggestions	39
REFERENCES	41
CURRICULUM VITAE	45

ABBREVIATIONS

<i>Or</i>	: Orbit or trajectory
tr	: Trace
det	: Determinant
Re	: Real part of a complex number
Im	: Imaginary part of a complex number
crit	: Critical value





SYMBOLS

\mathcal{X}	: State space or phase space
T	: Time set
t	: Time
Ψ^t	: Evolution operator
x_0	: Initial state or equilibrium of a dynamical system
x_i	: Any state of a dynamical system
S	: Invariant set
v	: Rotation with a constant velocity
σ_0	: Equilibrium of a nonlinear system in polar form
μ, μ_1, μ_2	: Bifurcation parameters
μ_0	: Critical value of the bifurcation parameter μ
A	: Jacobian matrix at the origin
λ_1, λ_2	: Eigenvalues
η	: Real part of a complex eigenvalue
ω	: Imaginary part of a complex eigenvalue
ω_0	: ω at the critical value of the bifurcation parameter
q, p	: Eigenvectors
O	: Order
F	: Taylor expansion starting with at least quadratic terms
g_{kl}	: Coefficient components of at least quadratic terms
B	: Quadratic terms of a nonlinear system
C	: Cubic terms of a nonlinear system
D	: Fourth-order terms of a nonlinear system
E	: Fifth-order terms of a nonlinear system
τ	: Linear time
θ	: Nonlinear time
l_1	: The first Lyapunov coefficient
l_2	: The second Lyapunov coefficient
G, U	: Control functions
$\beta_1, \beta_2, \beta_3$: Control parameters
u	: Share of labour in national income
v	: Proportion of labour force employment
ρ, φ	: Positive constants of the share equation
α	: Exogenous growth rate in labour productivity
γ	: Exogenous growth rate in labour force
ζ	: Capital-output ratio



LIST OF TABLES

	<u>Page</u>
Table 2.1 : Stability of the equilibrium $\sigma_0(\mu)$ at the origin.....	7





LIST OF FIGURES

	<u>Page</u>
Figure 3.1 : Solution curves and trajectories of the modified Goodwin model for $\lambda = 1$, $\rho = 0.05$, $k = 20.02$, $m = 0.002$, $\tilde{u} = 0.9$ with the initial condition $(0.0002002, -0.05005)$	24
Figure 3.2 : Solution curves and the phase portrait illustrating a focus corresponding to the bifurcation parameter $\mu_1 = -0.1$	28
Figure 3.3 : Solution curves and the phase portrait illustrating a weakly attracting focus corresponding to the bifurcation parameter $\mu_1 = 0$. .	28
Figure 3.4 : Solution curves and the phase portraits illustrating a stable limit cycle corresponding to the bifurcation parameter $\mu_1 = 0.01$	29
Figure 3.5 : Solution curves and the phase portrait illustrating a sole stable equilibrium without any limit cycle corresponding to the bifurcation parameters $\mu_1 = \mu_2 = 0$	32
Figure 3.6 : Solution curves and the phase portrait illustrating a sole stable equilibrium without any limit cycle corresponding to the bifurcation parameters $\mu_1 = 0$, $\mu_2 = -0.2$	33
Figure 3.7 : Solution curves and the phase portraits illustrating a sole stable equilibrium without any limit cycle corresponding to the bifurcation parameters $\mu_1 = -1$, $\mu_2 = 0.2$ in (a) and (b), $\mu_1 = -1$, $\mu_2 = 0$ in (c) and (d), $\mu_1 = -0.5$, $\mu_2 = -0.5$ in (e) and (f).	34
Figure 3.8 : Solution curves and the phase portraits illustrating the presence of a distinct stable limit cycle corresponding to the bifurcation parameters $\mu_1 = 0.0011$, $\mu_2 = -0.05$	35
Figure 3.9 : Solution curves and the phase portraits illustrating the presence of a distinct stable limit cycle corresponding to the bifurcation parameters $\mu_1 = 0$, $\mu_2 = 0.2$	36
Figure 3.10 : Solution curves illustrating the presence of two limit cycles corresponding to the bifurcation parameters $\mu_1 = -0.05$, $\mu_2 = 0.5$. ..	37



CONTROL OF HOPF AND BAUTIN BIFURCATION IN A MODIFIED GOODWIN MODEL OF GROWTH CYCLE

SUMMARY

In this thesis, we conduct a comprehensive analysis of regulating key bifurcation features, such as the stability of the equilibrium and the stability and orientation of the limit cycles, in Desai et al.'s modified Goodwin model of growth cycle, which elucidates the dynamics of class struggle in controlling economic systems. The study systematically manipulates model parameters to position the economy within the desired regions of both the Hopf and Bautin bifurcation diagrams.

The original Goodwin model comprises two dynamic equations:

$$\begin{aligned}\dot{u}(t) &= (\rho v(t) - (\alpha + \varphi))u(t), \\ \dot{v}(t) &= \left(\frac{1 - u(t)}{\zeta} - (\alpha + \gamma) \right) v(t)\end{aligned}$$

where $u(t)$ is the share of labour in national income, and $v(t)$ is the proportion of labour force employment. Solutions of the system exhibit clockwise closed cycles, each centered at the singular point (\tilde{u}, \tilde{v}) where

$$(\tilde{u}, \tilde{v}) = \left(1 - \zeta(\alpha + \gamma), \frac{\alpha + \varphi}{\rho} \right).$$

\tilde{u} may exceed one for $\alpha + \gamma < 0$ whereas it is inherently less than one for $\alpha + \gamma > 0$. Similarly, \tilde{v} may surpass one. It implies that the singular point (\tilde{u}, \tilde{v}) may extend beyond the unit area, leading to trajectories that partially or entirely exist outside that area. Even if the singular point remains within the unit box, trajectories could extend partially outside its boundaries. As a result, values surpassing one produce impractical outcomes for both the labour share and the employment rate. The modified Goodwin model proposed by Desai et al. satisfies this requirement, and all trajectories lie inside the unit square. This modified system is as follows

$$\begin{aligned}\dot{u} &= \rho \left((1 - v)^{-\delta} - k \right) u, \\ \dot{v} &= \lambda \left(\ln \frac{\tilde{u} - u}{1 - \tilde{u}} - m \right) v\end{aligned}$$

where $\delta = 1$, $k = \frac{\alpha + \varphi}{\rho}$ and $m = \frac{\alpha + \gamma}{\lambda}$.

The equilibrium (u_0, v_0) of this system is $\left(\tilde{u} - e^m(1 - \tilde{u}), 1 - \frac{1}{k}\right)$ and the substitutions $u \rightarrow X_1 - e^m(1 - \tilde{u}) + \tilde{u}$ and $v \rightarrow X_2 + 1 - \frac{1}{k}$ transform the equilibrium to the origin. The system takes the following form

$$\begin{aligned} H_1(X) &= \dot{X}_1 = -\rho k^2 \left(e^m(\tilde{u} - 1) + \tilde{u} + X_1 \right) \frac{X_2}{kX_2 - 1}, \\ H_2(X) &= \dot{X}_2 = \lambda \left(1 - \frac{1}{k} + X_2 \right) \left(-m + \ln \frac{e^m(1 - \tilde{u}) - X_1}{1 - \tilde{u}} \right). \end{aligned}$$

The Jacobian matrix of the modified system at the origin

$$\begin{pmatrix} 0 & \rho k^2 (e^m(\tilde{u} - 1) + \tilde{u}) \\ \frac{\lambda(k-1)}{ke^m(\tilde{u}-1)} & 0 \end{pmatrix}$$

has a pair of purely imaginary eigenvalues $\lambda_{1,2} = \pm i\omega_0$. An equilibrium with a pair of complex conjugate eigenvalues may lose its stability at a parameter exceeding a threshold value and transition to a small amplitude limit cycle called Hopf bifurcation. In the supercritical Hopf bifurcation, the limit cycle emerges at the bifurcation parameter greater than its critical value. In the subcritical Hopf bifurcation, the limit cycle is observed at the parameter values less than its critical value. The sign of the first Lyapunov coefficient at the critical value of the bifurcation parameter determines the type of the Hopf bifurcation. The second Lyapunov coefficient is evaluated where the first Lyapunov coefficient vanishes. The system undergoes another bifurcation, incorporating families of stable and unstable limit cycles coexisting, with one nested within the other, colliding, and eventually disappearing through a saddle-node bifurcation. It is called Bautin bifurcation, and it influences the stability of the equilibrium and the orientation of the resulting limit cycle. Understanding the behaviour of such systems is crucial, as they often exhibit fascinating bifurcation diagrams.

Recently, a range of control laws were proposed to manipulate the bifurcation features. In this study, we will utilise the control law offered by Braga et al. in 2010 to generate controllable Hopf and Bautin bifurcation. The control law depends on two bifurcation parameters $\mu_1, \mu_2 \in \mathbb{R}$ and four control parameters $\beta_1, \beta_2, \beta_3, \text{tr}(dG(0)) \in \mathbb{R}$.

Let us define the modified Goodwin model with the control law $G(X)U(X, \mu, \beta)$:

$$X_i' = H_i(X) + G_i(X)U(X, \mu, \beta), \quad i = 1, 2$$

where $\text{tr}(dG(0)) \neq 0$ and $U(X, \mu, \beta) = \beta_1\mu_1 + (\beta_2 + \mu_2)(X_1^2 + X_2^2) + \beta_3(X_1^2 + X_2^2)^2$. Its Jacobian matrix at the origin

$$\begin{pmatrix} \beta_1\mu_1 s & \rho k^2 (e^m(\tilde{u} - 1) + \tilde{u}) \\ \frac{\lambda(k-1)}{ke^m(\tilde{u}-1)} & \beta_1\mu_1 s \end{pmatrix}$$

gives a pair of complex conjugate eigenvalues $\lambda_{1,2} = \beta_1\mu_1 s \pm i\omega_0$.

The transversality condition of the Hopf bifurcation indicates that the derivative of the eigenvalue's real part with respect to the Hopf bifurcation parameter is non-zero. Considering that the Hopf bifurcation necessitates a pair of purely imaginary eigenvalues and the transversality condition, we fix the Hopf bifurcation parameter μ_1 to zero when evaluating the Lyapunov coefficients. We calculate the first and second Lyapunov coefficients as presented by Kuznetsov et al. The first and second Lyapunov coefficients of the modified Goodwin model with the control are, respectively,

$$l_1(0, \mu_2) = -\frac{2(\beta_2 + \mu_2)s \left(\lambda(1-k) + \rho k^3 e^m (\tilde{u}-1) (e^m (\tilde{u}-1) + \tilde{u}) \right)}{\lambda \omega_0 (k-1)}$$

and

$$l_2(0, 0) = \frac{2\beta_3 s}{\lambda^2 \omega_0 (k-1)^2} \left(3\lambda^2 (k-1)^2 - 2\lambda \rho k^3 (k-1) e^m (\tilde{u}-1) (e^m (\tilde{u}-1) + \tilde{u}) + 3\rho^2 k^6 e^{2m} (\tilde{u}-1)^2 (e^m (\tilde{u}-1) + \tilde{u})^2 \right).$$

The first Lyapunov coefficient vanishes at $\beta_{2\text{crit}}(\mu_2) = -\mu_2$, and the second Lyapunov coefficient is then calculated and vanishes at $\beta_3 = 0$.

Here, $\beta_{2\text{crit}}$ is the critical value of β_2 for which the first Lyapunov coefficient vanishes at the Hopf bifurcation parameter $\mu_1 = 0$; $\beta_{3\text{crit}}$ is the critical value of β_3 for which the second Lyapunov coefficient vanishes at the Bautin bifurcation parameters $\mu_1 = \mu_2 = 0$. Braga et al. state that the stability and the direction of the limit cycles emerging near the origin are controllable by selecting $\beta_1 \neq 0$, $\text{tr}(dG(0)) \neq 0$, $\beta_2 \neq \beta_{2\text{crit}}$ and $\beta_3 \neq \beta_{3\text{crit}}$.

Following Braga et al.'s control law, the control parameter values and the initial conditions are carefully selected. For various values of the bifurcation parameters μ_1 and μ_2 , all possible Hopf and Bautin bifurcation diagrams are plotted using NDSolve command of Mathematica, with a specified accuracy and precision goal of 10 digits. We observe that minor alterations in parameter values lead to variations in the behaviour of the modified model, resulting in different types of bifurcations.

Through this interdisciplinary analysis, we have advanced and expanded the findings regarding the Goodwin model's controllability and aimed to bridge theoretical insights with practical applications, thereby offering valuable contributions to policy decisions and strategic interventions to navigate the complexities of economic management.

This thesis is organised as follows. Chapter 1 includes the purpose of the study, literature review, and hypothesis research questions. In Chapter 2, bifurcation theory and stability in nonlinear dynamical systems are explained. The theorem and accompanying proof of both Hopf and Bautin bifurcation are given in Section 2.1 and Section 2.2, respectively. Section 2.3 introduces Braga et al.'s control law, and Section 2.4 presents the original Goodwin model and Desai et al.'s modified version. In Chapter 3, we perform the bifurcation analysis of the modified model for Hopf in Section 3.2 and Bautin in Section 3.3. Numerical simulations are also presented in this chapter. The last chapter is devoted to some concluding remarks and potential future studies.



DEĞİŞTİRİLMİŞ GOODWIN BÜYÜME DÖNGÜSÜ MODELİNDE HOPF VE BAUTIN ÇATALLANMASININ KONTROLÜ

ÖZET

Goodwin büyüme döngüsü modeli ilk olarak Richard M. Goodwin tarafından 1967'de öne sürülmüş, yıllar boyunca bilhassa matematikçiler ve ekonomistler tarafından ilgi görmüş ve çeşitli analizlere konu olmuştur. Lotka-Volterra'nın klasik av-avcı modeli esas alınarak tasarlanmıştır. Lotka-Volterra modelinde, av ve avcı popülasyonları arası etkileşimin zamana göre değişimi değerlendirilirken, Goodwin modelinde, istihdam oranı ve ücret payı gibi ekonomik dinamikler araştırılmaktadır.

Orijinal Goodwin modeli iki diferansiyel denklemden oluşur:

$$\begin{aligned}\dot{u}(t) &= \left(\rho v(t) - (\alpha + \varphi) \right) u(t), \\ \dot{v}(t) &= \left(\frac{1 - u(t)}{\zeta} - (\alpha + \gamma) \right) v(t).\end{aligned}$$

$u(t)$, emeğin milli gelirdeki payını ve $v(t)$, işgücü istihdam oranını temsil etmektedir. Sistemin çözümleri saat yönünde kapalı döngüler sergiler. Bu döngülerin merkezi (\tilde{u}, \tilde{v}) tekil noktasıdır:

$$(\tilde{u}, \tilde{v}) = \left(1 - \zeta(\alpha + \gamma), \frac{\alpha + \varphi}{\rho} \right).$$

Burada, \tilde{u} , $\alpha + \gamma$ 'nın negatif değerleri için 1'den büyük olabilirken, $\alpha + \varphi$ 'nin pozitif değerleri için 1'den küçüktür. Bu, \tilde{v} için de geçerlidir ve (\tilde{u}, \tilde{v}) merkezine sahip yörüngelerin bir kısmının veya tamamının birim alanın ötesine uzanabileceği anlamına gelmektedir. Tekil nokta alanın içinde yer alsa bile sistemin davranışını belirleyen yörüngelerin bir kısmı birim karenin sınırlarını aşabilir. Dolayısıyla, (\tilde{u}, \tilde{v}) 'nin 1'i aşan değerleri hem emek payı hem de istihdam oranı açısından elverişli olmayan sonuçlar doğurabilmektedir. Bu sorunu gidermek üzere literatürde çeşitli çalışmalar mevcuttur. Desai tarafından değiştirilmiş Goodwin modeli bu gereksinimi karşılar ve tüm yörüngeler birim karenin içinde yer alır. Bu model, $\delta = 1$, $k = \frac{\alpha + \varphi}{\rho}$ ve $m = \frac{\alpha + \gamma}{\lambda}$ olacak şekilde aşağıdaki gibidir:

$$\begin{aligned}\dot{u} &= \rho \left((1 - v)^{-\delta} - k \right) u, \\ \dot{v} &= \lambda \left(\ln \frac{\tilde{u} - u}{1 - \tilde{u}} - m \right) v.\end{aligned}$$

Bundan sonraki işlemler bu sistem için gerçekleştirilecektir.

İlk olarak, sistemin denge noktası $(u_0, v_0) = \left(\tilde{u} - e^m(1 - \tilde{u}), 1 - \frac{1}{k} \right)$, u yerine $X_1 - e^m(1 - \tilde{u}) + \tilde{u}$ ve v yerine $X_2 + 1 - \frac{1}{k}$ yazılarak orijine taşınır ve sistem aşağıdaki gibi şekillenir:

$$\begin{aligned} H_1(X) = \dot{X}_1 &= -\rho k^2 \left(e^m(\tilde{u} - 1) + \tilde{u} + X_1 \right) \frac{X_2}{kX_2 - 1}, \\ H_2(X) = \dot{X}_2 &= \lambda \left(1 - \frac{1}{k} + X_2 \right) \left(-m + \ln \frac{e^m(1 - \tilde{u}) - X_1}{1 - \tilde{u}} \right). \end{aligned}$$

Sistemin Jacobian matrisinin orijindeki değeri aşağıdaki gibidir:

$$\begin{pmatrix} 0 & \rho k^2 (e^m(\tilde{u} - 1) + \tilde{u}) \\ \frac{\lambda(k-1)}{ke^m(\tilde{u}-1)} & 0 \end{pmatrix}$$

Bu matris bir çift tamamen imajiner özdeğere sahiptir:

$$\lambda_{1,2} = \pm i\omega_0.$$

Bir çift karmaşık eşlenik özdeğer ile denge, parametrenin kritik değerinde kararlılığını kaybedebilir ve Hopf çatallanması adı verilen küçük genlikli bir limit döngüsüne geçiş yapabilir. Bu limit döngüsü, çatallanma parametresinin, kritik değerinden büyük veya küçük olduğu değerlerde görülebilir. Limit döngüsünün ortaya çıktığı bölge, parametrenin kritik değerindeki birinci Lyapunov katsayısının işareti ile saptanmaktadır.

Birinci Lyapunov katsayısı sıfırlanır ve ardından ikinci Lyapunov katsayısı hesaplanırsa, sistemde başka bir çatallanma türü meydana gelir. Bu, bir arada var olan, biri diğerinin içinde yer alan, çarpışan ve sonunda bir eyer-düğüm çatallanmasıyla ortadan kaybolan kararlı ve kararsız limit döngülerini barındıran Bautin çatallanmasıdır. Bautin çatallanması, hem dengenin stabilitesinde hem de ortaya çıkan limit döngülerinin yönünde etkilidir. Bu tür sistemlerin davranışını belirleyebilmek çok önemlidir. Çünkü bu sistemler büyüleyici çatallanma diyagramları sergiler.

Son yıllarda çatallanma özelliklerinin manipülasyonu üzerine bir dizi kontrol yasası geliştirilmiştir. Bu çalışmada, kontrol edilebilir Hopf ve Bautin çatallanmaları gözlemleyebilmek için 2010'da Braga tarafından önerilen kontrol yasasını takip edeceğiz. Bu kontrol yasası iki çatallanma parametresi ve dört kontrol parametresine bağlı olacak şekilde tasarlanmıştır.

Desai tarafından değiştirilmiş Goodwin modeli, $\text{tr}(dG(0)) \neq 0$ ve $U(X, \mu, \beta) = \beta_1 \mu_1 + (\beta_2 + \mu_2)(X_1^2 + X_2^2) + \beta_3(X_1^2 + X_2^2)^2$ olacak şekilde aşağıdaki sisteme dönüşür:

$$X_i' = H_i(X) + G_i(X)U(X, \mu, \beta), \quad i = 1, 2.$$

$\mu_1, \mu_2 \in \mathbb{R}$ çatallanma parametreleri ve $\beta_1, \beta_2, \beta_3, \text{tr}(dG(0)) \in \mathbb{R}$ kontrol parametreleridir.

Kontrol yasası uygulanmış yeni sistemin orijindeki Jacobian matrisi şu şekildedir:

$$\begin{pmatrix} \beta_1 \mu_1 s & \rho k^2 (e^m(\tilde{u}-1) + \tilde{u}) \\ \frac{\lambda(k-1)}{ke^m(\tilde{u}-1)} & \beta_1 \mu_1 s \end{pmatrix}$$

Bu matris ise reel kısmı sıfırdan farklı olan bir çift karmaşık eşlenik özdeğere sahiptir:

$$\lambda_{1,2} = \beta_1 \mu_1 s \pm i\omega_0.$$

Beklenen stabilite geçişi, özdeğerlerin reel kısmının çatallanma parametresine göre türevinin sıfırdan farklı olmasını gerektirir. Bu koşul ile Hopf çatallanmasına uğrayan bir sistemin tamamen imajiner özdeğere sahip olduğu gerçeği göz önüne alınarak, Lyapunov katsayıları hesaplanırken Hopf çatallanma parametresi μ_1 sifira sabitlenir.

Birinci ve ikinci Lyapunov katsayılarını hesaplarırken Kuznetsov'un çatallanma teorisine dair kitabındaki adımları takip ettiğimizi belirtmek isteriz. Bu doğrultuda, birinci Lyapunov katsayısı

$$l_1(0, \mu_2) = -\frac{2(\beta_2 + \mu_2)s \left(\lambda(1-k) + \rho k^3 e^m(\tilde{u}-1)(e^m(\tilde{u}-1) + \tilde{u}) \right)}{\lambda \omega_0(k-1)}$$

ve ikinci Lyapunov katsayısı

$$l_2(0, 0) = \frac{2\beta_3 s}{\lambda^2 \omega_0(k-1)^2} \left(3\lambda^2(k-1)^2 - 2\lambda \rho k^3(k-1)e^m(\tilde{u}-1)(e^m(\tilde{u}-1) + \tilde{u}) + 3\rho^2 k^6 e^{2m}(\tilde{u}-1)^2 (e^m(\tilde{u}-1) + \tilde{u})^2 \right)$$

olarak hesaplanır.

Hopf çatallanması μ_1 parametresine bağlıdır. $\mu_1 = 0$ 'da birinci Lyapunov katsayısı hesaplanır. Bautin çatallanması ise μ_1 ve μ_2 parametrelerine bağlı olarak gerçekleşir. $\mu_1 = \mu_2 = 0$ 'da ikinci Lyapunov katsayısı hesaplanır. İkinci Lyapunov katsayısının elde edilebilmesi için öncelikle birinci Lyapunov katsayısının sıfırlanması gerekmektedir.

Braga'nın kontrol sisteminde, β_2 'nin kritik değeri $\beta_{2\text{crit}}$, birinci Lyapunov katsayısının $\mu_1 = 0$ 'daki değerini sıfırlarken, β_3 'ün kritik değeri $\beta_{3\text{crit}}$ ise, ikinci Lyapunov katsayısının $\mu_1 = \mu_2 = 0$ 'daki değerini sıfırlamaktadır. Böylelikle, Desai'nin kontrol yasası eklenmiş Goodwin sisteminde birinci Lyapunov katsayısı, $\beta_{2\text{crit}}(\mu_2) = -\mu_2$ iken sıfırlanır ve ardından ikinci Lyapunov katsayısı hesaplanır. İkinci Lyapunov katsayısını sifira eşitleyen değer ise $\beta_{3\text{crit}} = 0$ değeridir.

Braga, β_1 'in sıfırdan ve β_2 'nin $\beta_{2\text{crit}}$ değerinden farklı olacak şekilde belirlenerek Hopf çatallanmasının kontrol altına alınabileceğini belirtmektedir. Bautin çatallanmasının kontrolü için ise β_1 ve $\text{tr}(dG(0))$ sıfırdan ve β_3 değeri $\beta_{3\text{crit}}$ değerinden farklı olacak şekilde seçilebilmektedir.

Çalışmamızda kontrol parametrelerinin değerleri ve başlangıç koşulları özenle belirlenmiş ve çatallanma parametreleri μ_1 ve μ_2 'nin çeşitli değerleri için tüm olası Hopf ve Bautin çatallanma diyagramları Mathematica'nın NDSolve komutu kullanılarak çizilmiştir. Parametre değerlerinde yapılan ufak değişiklikler, sistemin davranışında önemli değişimlere yol açabilmekte ve farklı çatallanma türlerinin oluşmasına sebep olabilmektedir.

Bu çalışma, sınıf mücadelesinin dinamiklerini belirleyen Desai tarafından değiştirilmiş Goodwin büyüme döngüsü modelinde, denge noktasının kararlılığı ve limit döngülerinin kararlılığı/yönü gibi temel çatallanma özelliklerinin düzenlenmesine ilişkin kapsamlı bir analizi içermektedir. Ekonomik dinamikleri Hopf ve Bautin çatallanma diyagramlarında arzu edilen bölgelere konumlandırmak için model parametrelerinin sistematik manipülasyonuna odaklanmaktadır.

Analiz, Goodwin modelinin kontrol edilebilirliğine ilişkin bulguları geliştirmiş ve genişletmiştir. Böylelikle, çatallanma teorisinin teorik temellerine ve ekonomideki uygulamalarına yönelik ileri araştırmalar gerçekleştirilebilecek, uygun politika kararları ve stratejik müdahaleler ile ekonomi yönetimindeki sorunlar iyileştirilebilecektir.

Bölüm 1'de, tezin amacı belirtilmiş, literatür taraması yapılmış ve hipotez araştırma soruları belirlenmiştir. Bölüm 2'de, lineer olmayan dinamik sistemler için çatallanma teorisi ve stabilite analizi anlatılmaktadır. Bölüm 2.1'de Hopf ve Bautin çatallanmasına yol açan koşullar irdelenmektedir. Bölüm 2.2'de Braga tarafından önerilen kontrol yasası, Bölüm 2.3'te orijinal Goodwin modeli ve Desai tarafından değiştirilmiş versiyonu tanıtılmaktadır. Bölüm 3'te, değiştirilmiş modelin Hopf ve Bautin çatallanması analizi gerçekleştirilmiş ve ilgili simülasyonlar sunulmuştur. Son bölüm sonuç değerlendirmelerine ve gelecekteki potansiyel çalışmalara ayrılmıştır.

1. INTRODUCTION

1.1 Purpose of Thesis

This thesis aims to conduct a comprehensive analysis of controlling Hopf bifurcations on the modified version of the classical Goodwin model by Desai et al. in 2006, focusing on determining the dynamics of class struggle in controlling economic systems. The investigation aims to systematically manipulate model parameters to position the economy within the desired regions of both Hopf and Bautin (the generalised Hopf) bifurcation diagrams. Additionally, the purpose involves developing the necessary steps to identify conditions for producing controllable Hopf and Bautin bifurcation by employing a specific control law proposed by Braga et al. in 2010.

1.2 Literature Review

Goodwin model of growth cycle [1], put forward by Richard M. Goodwin in 1967, was rooted in the classical Lotka-Volterra predator-prey model, as outlined in works by Lotka [2] and Volterra [3]. Both models explore the dynamics of groups. Dynamic equations of the Goodwin model formulate time-dependent potential states of economic activities such as capital, wages, unemployment, and labour and have been the subject of various analyses by mathematicians and economists over the years. Focusing on the interplay between inflation and unemployment, Desai's study [4] elaborates on the classical Goodwin model to examine the actual price inflation, its expected state, and the overcapacity. Contrary to customary analyses, Wolfstetter coherently interprets and evaluates short-term fluctuations arising from income and employment dynamics [5]. Ploeg examines the relevant models in detail [6]. Choi explores the implications of the Goodwin system undergoing a Hopf bifurcation, specifically considering scenarios where employee exertion depends on the real wage [7]. Foley obtains a growth model with capital, labour, and land inputs, combining several models, including Goodwin's, and receives results that underline land pricing

[8]. Tavani and Zamparelli study the role of policy-making in structuring the economy through a government sector change and the impact of public capital accumulation on employment, wage growth, labour productivity, and share [9]. Atkinson examines three diverse economic development models, taking into account the time scale and its relevance to the real economy, whether it is distinct or obscure [10].

An extension of the Goodwin model that aims to regulate its dynamics to confine the state variables within the unit square is introduced by Harvie et al. [11]. A similar attempt is also undertaken in [12]. One of the main assumptions in the Goodwin model of non-saving behaviour among workers is relaxed in [13] by incorporating the proportion of capital owned by workers as an additional variable. By introducing variable capacity utilisation and actual capital coefficients, Glombowski et al. formulate a four-dimensional model encompassing Goodwin's framework as a specific case [14]. Based on Minsky's financial instability hypothesis, Minsky and Keen integrate a banking sector into the Goodwin model of growth cycle [15, 16]. Consequently, the long-term existence of stable limit cycles in the model becomes uncertain, potentially leading to instabilities. The stability assessment of the model in [16] is conducted by Grasselli et al. in 2012 [17], while Grasselli et al. [18] further analyse the same dynamics in 2015. They incorporate an inflation term and construct a four-dimensional system that covers the flow of speculative money into the economy. Tebaldi et al. introduce modifications to the Goodwin model by changing the assumption of technical progress and introducing a memory variable that influences the behaviour of both workers and capitalists [19]. The proposed model exhibits a Hopf bifurcation at a critical value associated with the memory effect. In the realm of delayed dynamical systems, [20] is worth mentioning as it investigates the finite time delays between investment orders and the delivery of finished capital goods, coupled with a delayed response of real wages to unemployment levels.

A range of control systems were developed to generate different types of bifurcation and to regulate key bifurcation features such as the stability of the equilibrium and the stability and orientation of the limit cycles [21–26]. Hamzi et al. focus on the local bifurcations rather than the global bifurcations and work on the analysis and control of the Hopf bifurcation in [21]. Verduzco et al. reduce the analysis to the second dimension with the center manifold theory and derive the necessary conditions

to control the Hopf bifurcation [22]. Wen et al. present a control law to develop a desirable oscillatory behaviour in the high-dimensional systems by the center manifold theory and the normal form reduction [23]. They carry out the applications on an eight-dimensional chaotic system. Braga et al. aim to control the Hopf bifurcation in the linear systems [24] and the nonlinear systems [25]. Braga et al. design a control law depending on two bifurcation parameters and four control parameters in [26] and determine the conditions to control both Hopf and Bautin bifurcation in the nonlinear systems. In our study, we will utilise this control law [26] to regulate the bifurcation features in a modified Goodwin model.

1.3 Hypothesis & Research Questions

The hypothesis of this study posits that through systematic manipulation of model parameters and application of appropriate control strategies, it is possible to position an economic system within the desired regions of both Hopf and Bautin bifurcation diagrams. Specifically, it is expected that by employing the control law proposed by Braga et al. [26], controllable Hopf and Bautin bifurcation can be induced in the modified version of the classical Goodwin model presented by Desai et al. [27], thus enabling effective management of dynamics related to class struggle in economic systems.

The research questions can be summarized as follows.

1. How does systematic manipulation of model parameters influence the positioning of an economic system within desired regions of Hopf and Bautin bifurcation diagrams?
2. What essential conditions are required to induce controllable Hopf and Bautin bifurcation in the modified version of the classical Goodwin model?
3. How effective is Braga et al.'s control law [26] in managing dynamics related to class struggle within economic systems?



2. NONLINEAR DYNAMICAL SYSTEMS, STABILITY AND CONTROL

A dynamical system is a formulation of all potential states related to a phenomenon, including an initial condition and its progress over time. The set of all possible states is defined as the state space or phase space. The fundamental concepts related to the system in consideration are determined at the beginning of the analysis and remain unchanged throughout the analysis. Through this approach, we predict the time-dependent behaviour of the system within the context of predefined principles and frameworks.

In a dynamical system, we can distinguish between two kinds of time: continuous (real) time and discrete (integer) time. Orbits of a continuous-time dynamical system are continuous curves in the state space oriented by its direction of increase. These orbits reflect the system's evolution as time progresses. On the other hand, orbits of a discrete-time dynamical system are sequences of points in the state space enumerated by increasing integers. Unlike continuous-time orbits forming continuous curves, orbits in discrete-time systems are typically represented as discrete sequences advancing in discrete steps as time progresses. Let us define an orbit, also called a trajectory, starting at the initial state x_0 as an ordered subset of the state space \mathcal{X} :

$$Or(x_0) = \{x \in \mathcal{X} : x = \psi^t x_0, \forall t \in T\}$$

where the map $\psi^t : \mathcal{X} \rightarrow \mathcal{X}$ is the evolution operator parameterised by the time. Note that ψ^t transforms the initial state $x_0 \in \mathcal{X}$ into a state $x_t \in \mathcal{X}$ where $x_t = \psi^t x_0$. Let $x_0 \in \mathcal{X}$ be an equilibrium where $x_0 = \psi^t x_0$ for all $t \in T$. The equilibrium is the most prevalent orbit used for the continuous-time systems. Another phrase, the fixed point, is used for the discrete-time systems. Another common orbit is a cycle. A cycle of a continuous-time dynamical system, in a neighborhood of which there are no other cycles, is called a limit cycle or an isolated closed orbit.

The phase portrait of a dynamical system is a partitioning of the state space into orbits. Consider a set $S \subset \mathcal{X}$ with the equilibrium $x_0 \in S$. The subset S , consisting of the

orbits of the dynamical system, is called an invariant set of the system and informs us about the behaviour of a dynamical system as the phase portrait. A system can always be restricted to its invariant set. Moreover, each orbit can be identified as an invariant set of the system. Equilibriums, fixed points, and cycles are the most common exemplifications of invariant sets. A stable invariant set attracts the orbits around it. The stability will be detailed in Section 2.1 by relating it to the bifurcation theory. [28]

2.1 Bifurcation Theory and Stability

A differential equation is mostly convenient to define a continuous-time dynamical system [28]. The evolution of the system is given by

$$\frac{dx_i}{dt} = \dot{x}_i = f_i(x_1, x_2, \dots, x_n, \mu), \quad i = 1, 2, \dots, n$$

where the velocities \dot{x}_i are the functions of the coordinates (x_1, x_2, \dots, x_n) .

Consider a system of two differential equations:

$$\begin{aligned} \dot{x}_1 &= f_1(x_1, x_2, \mu) = \mu x_1 - x_2 - x_1(x_1^2 + x_2^2), \\ \dot{x}_2 &= f_2(x_1, x_2, \mu) = x_1 + \mu x_2 - x_2(x_1^2 + x_2^2), \end{aligned} \quad (2.1)$$

depending on one parameter $\mu \in \mathbb{R}^1$. An equilibrium exists at the origin such that $\dot{x}_1 = 0$ and $\dot{x}_2 = 0$. The Jacobian matrix, composed of the partial derivatives of the system, at the equilibrium $(x_1, x_2) = (0, 0)$ has the eigenvalues $\lambda_{1,2}(\mu) = \mu \pm i$.

Now, let us introduce a complex variable $z = x_1 + ix_2$ where $\bar{z} = x_1 - ix_2$ and $|z|^2 = z\bar{z} = x_1^2 + x_2^2$. The derivative of z with respect to t

$$\begin{aligned} \dot{z} &= \frac{dz}{dt} \\ &= \frac{dx_1}{dt} + i \frac{dx_2}{dt} \\ &= \dot{x}_1 + i\dot{x}_2 \\ &= \mu x_1 - x_2 - x_1(x_1^2 + x_2^2) + i(x_1 + \mu x_2 - x_2(x_1^2 + x_2^2)) \\ &= \mu(x_1 + ix_2) + i(x_1 + ix_2) - (x_1 + ix_2)(x_1^2 + x_2^2) \\ &= (\mu + i)z - z|z|^2 \end{aligned}$$

results in the complex form of the system (2.1):

$$\dot{z} = (\mu + i)z - z|z|^2. \quad (2.2)$$

By the representation of $z = \sigma e^{i\nu}$,

$$\begin{aligned}\dot{z} &= (\mu + i)z - z|z|^2, \\ \dot{\sigma}e^{i\nu} + \sigma i\dot{\nu}e^{i\nu} &= (\mu + i)\sigma e^{i\nu} - \sigma e^{i\nu}|\sigma e^{i\nu}|^2 \\ &= \sigma e^{i\nu}(\mu + i - \sigma^2),\end{aligned}$$

we get

$$\dot{\sigma} = \sigma(\mu + i - \sigma^2 - i\nu).$$

By substituting $\dot{\nu} = 1$, the complex form (2.2) transforms into the polar form:

$$\begin{aligned}\dot{\sigma} &= \sigma(\mu - \sigma^2), \\ \dot{\nu} &= 1.\end{aligned}\tag{2.3}$$

Here, $\dot{\nu}$ represents a rotation with a constant velocity. Therefore, we can only take into account the first equation of (2.3) for the stability analysis. We note that $\sigma(\mu)$ is considered to be greater than or equal to zero since the stability requires a decreasing function that attracts trajectories towards the equilibrium at the origin. There exist two equilibrium points $\sigma_0(\mu) = 0$ and $\sigma_0(\mu) = \sqrt{\mu}$ such that $\dot{\sigma} = 0$. The equilibrium $\sigma_0(\mu) = \sqrt{\mu}$ is stable for all $\mu > 0$. The behaviour of the system (2.3) at the equilibrium $\sigma_0(\mu) = 0$ is in Table 2.1.

Table 2.1 : Stability of the equilibrium $\sigma_0(\mu)$ at the origin.

Bifurcation Parameter	Stability	Type of Equilibrium
$\mu < 0$	Linearly Stable	Stable Focus
$\mu = 0$	Nonlinearly Stable	Weakly Attracting Focus
$\mu > 0$	Linearly Unstable	Unstable Focus

As in the case above, a parameter exceeding a threshold value can alter the system's stability and lead to periodic solutions. For instance, an equilibrium of the system, manifesting as a pair of complex conjugate eigenvalues crossing the imaginary axis of the complex plane with a non-zero velocity, may lose its stability and transition to a small amplitude limit cycle. This phenomenon, called Hopf bifurcation, is revealed in two forms: supercritical and subcritical.

In the supercritical scenario, an unstable equilibrium is surrounded by a stable limit cycle. Conversely, in the subcritical Hopf bifurcation, a stable equilibrium is encircled by an unstable limit cycle. To classify the Hopf bifurcation, we need to examine the

sign of the first Lyapunov coefficient at the critical value of the bifurcation parameter [28,29]. We will address the details regarding the first Lyapunov coefficient in Section 2.1.1.

It is clear that the system (2.1) undergoes a supercritical Hopf bifurcation since the bifurcation occurs when the limit cycle emerges at the parameter values $\mu > 0$. When we change the sign of the nonlinear terms, this change would be reflected in the complex and polar forms of the system. In a system where the sign of the cubic terms is positive, the bifurcation is classified as subcritical because it occurs when the limit cycle emerges for $\mu < 0$.

2.1.1 Hopf bifurcation

In this section, we will explore the Hopf bifurcation as outlined in [28] using the subsequent theorem and accompanying proof.

Theorem 2.1.1 *Let f be a smooth function and consider a planar nonlinear system*

$$\dot{x} = f(x, \mu), \quad x = (x_1, x_2)^T \in \mathbb{R}^2 \quad (2.4)$$

which depends on the parameter $\mu \in \mathbb{R}^1$ and has a non-hyperbolic equilibrium at the origin with a pair of purely imaginary eigenvalues for all sufficiently small $|\mu|$:

$$\lambda_{1,2}(\mu) = \eta(\mu) \pm i\omega(\mu) \quad (2.5)$$

where $\eta(0) = 0$ and $\omega(0) = \omega_0 > 0$.

If the system satisfies the following conditions at the bifurcation parameter $\mu = 0$:

(h.i) $\eta'(0) \neq 0$,

(h.ii) $l_1(0) \neq 0$, where $l_1(\mu)$ is the first Lyapunov coefficient,

then, by a linear and nonlinear complex coordinate shift, a linear time scale, and a nonlinear time reparametrisation, the system can be transformed into the complex form

$$\dot{u} = (\kappa + i)u + s|u|^2u + O(\|u\|^4) \quad (2.6)$$

where $s = \text{sign}[l_1(0)] = \pm 1$.

Proof 2.1.1 Suppose that the system (2.4) is nonlinear. Let $A(\mu)$ be the Jacobian matrix at the equilibrium $x = 0$:

$$A(\mu) = df(0, \mu) = \begin{pmatrix} \frac{\partial \dot{x}_1}{\partial x_1} & \frac{\partial \dot{x}_1}{\partial x_2} \\ \frac{\partial \dot{x}_2}{\partial x_1} & \frac{\partial \dot{x}_2}{\partial x_2} \end{pmatrix} \Big|_{(x_1, x_2) = (0, 0)}$$

We use this approach to linearise a nonlinear system, providing an approximation for locally assessing the system's behaviour near its equilibrium. The planar nonlinear system (2.4) is then represented as

$$\dot{x} = A(\mu)x + F(x, \mu), \quad x = (x_1, x_2)^T \in \mathbb{R}^2. \quad (2.7)$$

F denotes a Taylor expansion that includes terms up to at least quadratic order, represented by $O(\|x\|^2)$. The eigenvalues of $A(\mu)$ are as follows

$$\lambda_{1,2}(\mu) = \eta(\mu) \pm i\omega(\mu)$$

where

$$\eta(\mu) = \frac{1}{2} \text{tr}(A) \quad \text{and} \quad \omega(\mu) = \frac{1}{2} \sqrt{4 \det(A) - (\text{tr}(A))^2}. \quad (2.8)$$

We set $\eta(0)$ to be zero and $\omega(0) = \omega_0$ to be greater than zero since the equilibrium of the system is defined as a non-hyperbolic equilibrium with a pair of purely imaginary eigenvalues where $\omega(0) > 0$. Suppose that $\eta'(0) \neq 0$ (*h.i.*):

$$\left. \frac{\partial \eta(\mu)}{\partial \mu} \right|_{\mu=0} \neq 0.$$

It is referred to as the transversality condition, which indicates the stability transition that leads the system to undergo a Hopf Bifurcation. The transversality condition, indicating that the eigenvalues will cross the imaginary axis with a non-zero velocity as the system parameters vary, is captured by the derivative of the real part of the eigenvalue with respect to the Hopf bifurcation parameter μ .

Let $q(\mu) = (q_1(\mu), q_2(\mu))^T$, $p(\mu) = (p_1(\mu), p_2(\mu))^T \in \mathbb{C}^2$ be the eigenvectors of $A(\mu)$ and $A^T(\mu)$ corresponding to the eigenvalues $\lambda_1(\mu) = \lambda(\mu)$ and $\lambda_2(\mu) = \bar{\lambda}(\mu)$, respectively:

$$A(\mu)q(\mu) = \lambda(\mu)q(\mu) \quad \text{and} \quad A^T(\mu)p(\mu) = \bar{\lambda}(\mu)p(\mu),$$

provided that $\langle p(\mu), q(\mu) \rangle = 1$. By assuming a linear relation between x and the real and imaginary parts of some complex variable z for all sufficiently small $|\mu|$, let us redefine $x = zq(\mu) + \bar{z}\bar{q}(\mu)$. The scalar product of $p(\mu)$ and x is

$$\begin{aligned} \langle p(\mu), x \rangle &= \langle p(\mu), zq(\mu) + \bar{z}\bar{q}(\mu) \rangle \\ &= \langle p(\mu), zq(\mu) \rangle + \langle p(\mu), \bar{z}\bar{q}(\mu) \rangle \\ &= z \langle p(\mu), q(\mu) \rangle + \bar{z} \langle p(\mu), \bar{q}(\mu) \rangle \\ &= z \end{aligned}$$

where $\langle p(\mu), q(\mu) \rangle = 1$ and $\langle p(\mu), \bar{q}(\mu) \rangle = 0$. The derivative of the last equation

$$\begin{aligned} \dot{z} &= \langle \dot{p}(\mu), x \rangle + \langle p(\mu), \dot{x} \rangle \\ &= \langle p(\mu), A(\mu)x + F(x, \mu) \rangle \\ &= \langle p(\mu), A(\mu)x \rangle + \langle p(\mu), F(x, \mu) \rangle \\ &= \langle A^T(\mu)p(\mu), x \rangle + \langle p(\mu), F(x, \mu) \rangle \\ &= \langle \bar{\lambda}(\mu)p(\mu), x \rangle + \langle p(\mu), F(x, \mu) \rangle \\ &= \lambda(\mu) \langle p(\mu), x \rangle + \langle p(\mu), F(x, \mu) \rangle \\ &= \lambda(\mu)z + \langle p(\mu), F(x, \mu) \rangle \end{aligned}$$

results in the following equation

$$\dot{z} = \lambda(\mu)z + \langle p(\mu), F(zq(\mu) + \bar{z}\bar{q}(\mu), \mu) \rangle. \quad (2.9)$$

Let g represent at least quadratic terms of \dot{z} :

$$\dot{z} = \lambda(\mu)z + g(z, \bar{z}, \mu)$$

where

$$\begin{aligned} g(z, \bar{z}, \mu) &= \langle p(\mu), F(zq(\mu) + \bar{z}\bar{q}(\mu), \mu) \rangle \\ &= \sum_{k+l \geq 2} \frac{1}{k!l!} g_{kl}(\mu) z^k \bar{z}^l, \\ g_{kl}(\mu) &= \left\{ \frac{\partial^{k+l}}{\partial z^k \partial \bar{z}^l} \langle p(\mu), F(zq(\mu) + \bar{z}\bar{q}(\mu), \mu) \rangle \right\} \Big|_{z=0} \end{aligned} \quad (2.10)$$

for $k+l \geq 2$ and $k, l = 0, 1, \dots$

Let us define $B = (B_1, B_2)^T$ and $C = (C_1, C_2)^T$ as symmetric multilinear vector-valued functions of $x, y, z \in \mathbb{R}^2$ as follows

$$B_i(x, y) = \sum_{j,k=1}^2 \frac{\partial^2 F_i(\xi)}{\partial \xi_j \partial \xi_k} \Big|_{\xi=0} x_j y_k, \quad i = 1, 2, \quad (2.11)$$

$$C_i(x, y, z) = \sum_{j,k,l=1}^2 \frac{\partial^3 F_i(\xi)}{\partial \xi_j \partial \xi_k \partial \xi_l} \Big|_{\xi=0} x_j y_k z_l, \quad i = 1, 2. \quad (2.12)$$

The expansion of B can be stated as

$$\begin{aligned} B_i(x, y) &= \sum_{j=1}^2 \sum_{k=1}^2 \frac{\partial^2 F_i(\xi_1, \xi_2)}{\partial \xi_j \partial \xi_k} \Big|_{(\xi_1, \xi_2)=(0,0)} x_j y_k \\ &= \sum_{j=1}^2 \left\{ \frac{\partial^2 F_i(\xi_1, \xi_2)}{\partial \xi_j \partial \xi_1} x_j y_1 + \frac{\partial^2 F_i(\xi_1, \xi_2)}{\partial \xi_j \partial \xi_2} x_j y_2 \right\} \Big|_{\xi=0} \\ &= \left\{ \frac{\partial^2 F_i(\xi_1, \xi_2)}{\partial \xi_1 \partial \xi_1} x_1 y_1 + \frac{\partial^2 F_i(\xi_1, \xi_2)}{\partial \xi_2 \partial \xi_1} x_2 y_1 + \frac{\partial^2 F_i(\xi_1, \xi_2)}{\partial \xi_1 \partial \xi_2} x_1 y_2 + \frac{\partial^2 F_i(\xi_1, \xi_2)}{\partial \xi_2 \partial \xi_2} x_2 y_2 \right\} \Big|_{\xi=0}. \end{aligned}$$

We then conclude

$$B_i(x, x) = \frac{\partial^2 F_i(0, 0)}{\partial x_1^2} x_1^2 + 2 \left(\frac{\partial^2 F_i(0, 0)}{\partial x_1 \partial x_2} x_1 x_2 \right) + \frac{\partial^2 F_i(0, 0)}{\partial x_2^2} x_2^2, \quad i = 1, 2. \quad (2.13)$$

Similarly, by using the expansion of C , we obtain

$$C_i(x, x, x) = \frac{\partial^3 F_i(0, 0)}{\partial x_1^3} x_1^3 + \frac{\partial^3 F_i(0, 0)}{\partial x_1^2 \partial x_2} x_1^2 x_2 + \frac{\partial^3 F_i(0, 0)}{\partial x_1 \partial x_2^2} x_1 x_2^2 + \frac{\partial^3 F_i(0, 0)}{\partial x_2^3} x_2^3, \quad i = 1, 2. \quad (2.14)$$

We note that $F = F(x, \mu)$ is defined as a Taylor expansion beginning with the terms of at least quadratic order. By the expansion of F at $\mu = 0$, we get

$$\begin{aligned} F_i(x, 0) &= \frac{1}{2} \left\{ \frac{\partial^2 F_i(0, 0)}{\partial x_1^2} x_1^2 + 2 \left(\frac{\partial^2 F_i(0, 0)}{\partial x_1 \partial x_2} x_1 x_2 \right) + \frac{\partial^2 F_i(0, 0)}{\partial x_2^2} x_2^2 \right\} + \\ &\quad \frac{1}{6} \left\{ \frac{\partial^3 F_i(0, 0)}{\partial x_1^3} x_1^3 + \frac{\partial^3 F_i(0, 0)}{\partial x_1^2 \partial x_2} x_1^2 x_2 + \frac{\partial^3 F_i(0, 0)}{\partial x_1 \partial x_2^2} x_1 x_2^2 + \frac{\partial^3 F_i(0, 0)}{\partial x_2^3} x_2^3 \right\} + \\ &\quad O(\|x\|^4), \quad i = 1, 2. \end{aligned}$$

Clearly, $B_i(x, x)$ and $C_i(x, x, x)$ refer to the quadratic and cubic terms of $F_i(x, 0)$, respectively:

$$F_i(x, 0) = \frac{1}{2} B_i(x, x) + \frac{1}{6} C_i(x, x, x) + O(\|x\|^4), \quad i = 1, 2. \quad (2.15)$$

We have demonstrated the relationship between B , C and F .

F can also be expressed as follows

$$\begin{aligned} F_i(x, 0) &= F_i(x_1, x_2, 0) \\ &= F_i(zq_1 + \bar{z}\bar{q}_1, zq_2 + \bar{z}\bar{q}_2, 0), \quad i = 1, 2 \end{aligned} \quad (2.16)$$

where $q(\mu) = q$ at $\mu = 0$. The partial derivative of (2.16) with respect to \bar{z} , and the second-order partial derivative with respect to \bar{z} and z , respectively, are

$$\begin{aligned} \frac{\partial F_i(x, 0)}{\partial \bar{z}} &= \frac{\partial F_i(x_1, x_2, 0)}{\partial \bar{z}} \\ &= \frac{\partial F_i(x_1, x_2, 0)}{\partial x_1} \frac{\partial x_1}{\partial \bar{z}} + \frac{\partial F_i(x_1, x_2, 0)}{\partial x_2} \frac{\partial x_2}{\partial \bar{z}} \\ &= \frac{\partial F_i(x_1, x_2, 0)}{\partial x_1} \bar{q}_1 + \frac{\partial F_i(x_1, x_2, 0)}{\partial x_2} \bar{q}_2, \\ \frac{\partial^2 F_i(x, 0)}{\partial z \partial \bar{z}} &= \frac{\partial}{\partial z} \left(\frac{\partial F_i(x_1, x_2, 0)}{\partial x_1} \bar{q}_1 + \frac{\partial F_i(x_1, x_2, 0)}{\partial x_2} \bar{q}_2 \right) \\ &= \frac{\partial}{\partial z} \left(\frac{\partial F_i(x_1, x_2, 0)}{\partial x_1} \right) \bar{q}_1 + \frac{\partial}{\partial z} \left(\frac{\partial F_i(x_1, x_2, 0)}{\partial x_2} \right) \bar{q}_2 \\ &= \left(\frac{\partial^2 F_i(x_1, x_2, 0)}{\partial x_1^2} \frac{\partial x_1}{\partial z} \right) \bar{q}_1 + \\ &\quad \left(\frac{\partial^2 F_i(x_1, x_2, 0)}{\partial x_1 \partial x_2} \frac{\partial x_2}{\partial z} \right) \bar{q}_1 + \left(\frac{\partial^2 F_i(x_1, x_2, 0)}{\partial x_2 \partial x_1} \frac{\partial x_1}{\partial z} \right) \bar{q}_2 + \\ &\quad \left(\frac{\partial^2 F_i(x_1, x_2, 0)}{\partial x_2^2} \frac{\partial x_2}{\partial z} \right) \bar{q}_2 \\ &= \frac{\partial^2 F_i(x_1, x_2, 0)}{\partial x_1^2} q_1 \bar{q}_1 + \\ &\quad \frac{\partial^2 F_i(x_1, x_2, 0)}{\partial x_1 \partial x_2} (q_2 \bar{q}_1 + q_1 \bar{q}_2) + \\ &\quad \frac{\partial^2 F_i(x_1, x_2, 0)}{\partial x_2^2} q_2 \bar{q}_2. \end{aligned}$$

We then obtain the following equality

$$\frac{\partial^2 F_i(x, 0)}{\partial z \partial \bar{z}} = \frac{\partial^2 F_i(zq + \bar{z}\bar{q}, 0)}{\partial z \partial \bar{z}} = B_i(q, \bar{q}), \quad i = 1, 2. \quad (2.17)$$

The definition of g_{kl} in (2.10) enables us to express $g_{kl}(0)$ using the equation (2.17) as

$$g_{11}(0) = \langle p, B_i(q, \bar{q}) \rangle, \quad i = 1, 2$$

where $k, l = 1$. Similarly, by using the partial derivative of (2.16) with respect to z and z , we get

$$g_{20}(0) = \langle p, B_i(q, q) \rangle, \quad i = 1, 2$$

where $k = 2$ and $l = 0$; and by using the partial derivative of (2.16) with respect to \bar{z} and \bar{z} , we obtain

$$g_{02}(0) = \langle p, B_i(\bar{q}, \bar{q}) \rangle, \quad i = 1, 2$$

where $k = 0$ and $l = 2$. We have represented all relevant g_{kl} 's with respect to B for $k + l = 2$. Likewise, the relevant expressions of g_{kl} in terms of C for $k + l = 3$ are as follows

$$g_{30}(0) = \langle p, C_i(q, q, q) \rangle, \quad k = 3, \quad l = 0, \quad i = 1, 2,$$

$$g_{21}(0) = \langle p, C_i(q, q, \bar{q}) \rangle, \quad k = 2, \quad l = 1, \quad i = 1, 2,$$

$$g_{12}(0) = \langle p, C_i(q, \bar{q}, \bar{q}) \rangle, \quad k = 1, \quad l = 2, \quad i = 1, 2,$$

$$g_{03}(0) = \langle p, C_i(\bar{q}, \bar{q}, \bar{q}) \rangle, \quad k = 0, \quad l = 3, \quad i = 1, 2.$$

Ultimately, our goal is to eliminate the quadratic and cubic terms of (2.9) by employing a nonlinear complex coordinate shift, thus reducing its complexity. First, let us express \dot{z} based on the results above:

$$\begin{aligned} \dot{z} &= \lambda z + \sum_{2 \leq k+l \leq 3} \frac{1}{k!l!} g_{kl}(\mu) z^k \bar{z}^l + O(\|z\|^4) \\ &= \lambda z + \frac{g_{20}}{2} z^2 + g_{11} z \bar{z} + \frac{g_{02}}{2} \bar{z}^2 + \frac{g_{30}}{6} z^3 + \frac{g_{21}}{2} z^2 \bar{z} + \frac{g_{12}}{2} z \bar{z}^2 + \frac{g_{03}}{6} \bar{z}^3 + O(\|z\|^4), \end{aligned}$$

then introduce an integrated nonlinear complex coordinate depending on an invertible parameter w to eliminate both the quadratic and cubic terms:

$$\begin{aligned} z &= w + \sum_{2 \leq k+l \leq 3} \frac{1}{k!l!} h_{kl}(\mu) w^k \bar{w}^l \\ &= w + \frac{h_{20}}{2} w^2 + h_{11} w \bar{w} + \frac{h_{02}}{2} \bar{w}^2 + \frac{h_{30}}{6} w^3 + \frac{h_{21}}{2} w^2 \bar{w} + \frac{h_{12}}{2} w \bar{w}^2 + \frac{h_{03}}{6} \bar{w}^3. \end{aligned}$$

The inverse change of variable gives

$$w = z - \frac{h_{20}}{2} z^2 - h_{11} z \bar{z} - \frac{h_{02}}{2} \bar{z}^2 - \frac{h_{30}}{6} z^3 - \frac{h_{21}}{2} z^2 \bar{z} - \frac{h_{12}}{2} z \bar{z}^2 - \frac{h_{03}}{6} \bar{z}^3 + O(\|z\|^4).$$

The derivative of w is expressed as

$$\begin{aligned} \dot{w} &= \dot{z} - h_{20} z \dot{z} - h_{11} (\dot{z} \bar{z} + z \dot{\bar{z}}) - h_{02} \bar{z} \dot{\bar{z}} - \\ &\quad \frac{h_{30}}{2} z^2 \dot{z} - \frac{h_{21}}{2} (2z \bar{z} \dot{z} + z^2 \dot{\bar{z}}) - \frac{h_{12}}{2} (\dot{z} \bar{z}^2 + 2z \bar{z} \dot{\bar{z}}) - \frac{h_{03}}{2} \bar{z}^2 \dot{\bar{z}} + O(\|z\|^4). \end{aligned}$$

Substituting z and \dot{z} in \dot{w} , and then expressing each h_{kl} by the relevant g_{kl} , eliminates the coefficients of the quadratic and cubic terms. The ultimate equation is as follows

$$\dot{w} = \lambda(\mu)w + c_1(\mu)w^2 \bar{w} + O(\|w\|^4) \quad (2.18)$$

where

$$c_1(\mu) = \frac{g_{20}g_{11}(2\lambda(\mu) + \bar{\lambda}(\mu))}{2|\lambda(\mu)|^2} + \frac{|g_{11}|^2}{\lambda(\mu)} + \frac{|g_{02}|^2}{2(2\lambda(\mu) - \bar{\lambda}(\mu))} + \frac{g_{21}}{2}.$$

We recall that $\lambda(\mu) = \eta(\mu) + i\omega(\mu)$ where $\eta(0) = 0$ and $\omega(0) = \omega_0 > 0$. Indeed,

$$c_1(0) = \frac{i}{2w_0} \left(g_{20}g_{11} - 2|g_{11}|^2 - \frac{1}{3}|g_{02}|^2 \right) + \frac{g_{21}}{2} \neq 0$$

where $\lambda(0) = i\omega_0$.

We have eliminated all the quadratic terms and all but one of the cubic terms. Although we can not set the coefficient of the resonant cubic term to zero, we can reduce it by a linear time scale, a nonlinear time reparametrisation, and a nonlinear complex coordinate shift. Let us begin by introducing a linear time variable. Since $\omega(0) = \omega_0 > 0$ and $\omega(\mu)$ is continuous, $\omega(\mu)$ is greater than zero for all sufficiently small $|\mu|$. Then, we can define the linear time variable as $\tau = \omega(\mu)t$. By this definition, we get

$$\frac{d}{dt} = \frac{d}{d\tau} \frac{d\tau}{dt} = \omega(\mu) \frac{d}{d\tau} \quad \text{and} \quad \dot{w} = \frac{dw}{dt} = \omega(\mu) \frac{dw}{d\tau}.$$

The equation (2.18) then transforms into the following expression

$$\frac{dw}{d\tau} = (\kappa(\mu) + i)w + \frac{c_1(\mu)}{\omega(\mu)}|w|^2w + O(\|w\|^4) \quad (2.19)$$

where $\kappa(\mu) = \frac{\eta(\mu)}{\omega(\mu)}$.

$\kappa = \kappa(\mu)$ is a new parameter satisfying

$$\kappa(0) = \frac{\eta(0)}{\omega(0)} = 0, \quad \kappa'(0) = \frac{\eta'(0)\omega(0) - \eta(0)\omega'(0)}{(\omega(0))^2} = \frac{\eta'(0)}{\omega(0)} \neq 0.$$

We can express the equation (2.19) in terms of the parameter κ as

$$\frac{dw}{d\tau} = (\kappa + i)w + d_1(\kappa)|w|^2w + O(\|w\|^4) \quad (2.20)$$

where $d_1(\kappa) = \frac{c_1(\mu(\kappa))}{\omega(\mu(\kappa))}$. Notice that the coefficient $d_1(\kappa)$ is complex.

Now, we will introduce a nonlinear time variable $\theta = \theta(\tau, \kappa)$ where

$$d\theta = (1 + e_1(\kappa)|w|^2)d\tau, \quad e_1(\kappa) = \text{Im}[d_1(\kappa)].$$

Then, it follows that

$$\frac{d}{d\tau} = \frac{d}{d\theta} \frac{d\theta}{d\tau} = (1 + e_1(\kappa)|w|^2) \frac{d}{d\theta}$$

and

$$\begin{aligned}\frac{dw}{d\theta} &= \frac{1}{1 + e_1(\kappa)|w|^2} ((\kappa + i)w + d_1(\kappa)|w|^2w + O(\|w\|^4)) \\ &= (1 - e_1(\kappa)|w|^2) ((\kappa + i)w + d_1(\kappa)|w|^2w + O(\|w\|^4)) \\ &= (\kappa + i)w + (d_1(\kappa) - (\kappa + i)e_1(\kappa))|w|^2w + O(\|w\|^4).\end{aligned}$$

The equation (2.20) then reduces to the following

$$\frac{dw}{d\theta} = (\kappa + i)w + l_1(\kappa)|w|^2w + O(\|w\|^4) \quad (2.21)$$

where $l_1(\kappa) = d_1(\kappa) - (\kappa + i)e_1(\kappa)$ is the first Lyapunov coefficient. Let $d_1(\kappa)$ be complex, decomposed into its real part a and imaginary part b . Then, $e_1(\kappa) = \text{Im}[d_1(\kappa)] = b$ and

$$\begin{aligned}l_1(\kappa) &= d_1(\kappa) - (\kappa + i)e_1(\kappa) \\ &= a + bi - (\kappa + i)b \\ &= a - \kappa b \\ &= \text{Re}[d_1(\kappa)] - \kappa \text{Im}[d_1(\kappa)].\end{aligned}$$

We note that the coefficient $l_1(\kappa)$ is real while the coefficient $d_1(\kappa)$ is complex. At $\kappa = 0$, we get

$$\begin{aligned}l_1(0) &= \text{Re}[d_1(0)] - \kappa \text{Im}[d_1(0)] \\ &= \text{Re} \left[\frac{c_1(\mu(0))}{\omega(\mu(0))} \right] \\ &= \frac{\text{Re}[c_1(0)]}{\omega_0}.\end{aligned} \quad (2.22)$$

Therefore, the first Lyapunov coefficient at the origin is given by

$$l_1(0) = \frac{1}{2\omega_0^2} \text{Re} \left[ig_{20}g_{11} + \omega_0 g_{21} \right]. \quad (2.23)$$

Let us introduce a linear complex coordinate u

$$w = \frac{u}{\sqrt{|l_1(\kappa)|}} \quad (2.24)$$

where $l_1(0) = \text{Re}[c_1(0)] \neq 0$. It satisfies the condition (h.ii). Using the complex variable u , the equation (2.21) yields

$$\begin{aligned}\frac{dw}{d\theta} &= \frac{1}{\sqrt{|l_1(\kappa)|}} \frac{du}{d\theta} \\ &= (\kappa + i) \frac{u}{\sqrt{|l_1(\kappa)|}} + l_1(\kappa) \frac{|u|^2}{|l_1(\kappa)|} \frac{u}{\sqrt{|l_1(\kappa)|}} + O(\|u\|^4)\end{aligned}$$

and

$$\begin{aligned}\frac{du}{d\theta} &= (\kappa + i)u + \frac{l_1(\kappa)}{|l_1(\kappa)|} |u|^2 u + O(\|u\|^4) \\ &= (\kappa + i)u + s|u|^2 u + O(\|u\|^4)\end{aligned}\tag{2.25}$$

where $s = \text{sign}[l_1(0)] = \text{sign}[\text{Re}[c_1(0)]] = \pm 1$.

By following each step outlined in Theorem 2.1.1, we have successfully simplified the coefficient of the resonant cubic term, resulting in the complex form (2.25) of the system (2.4). \square

2.1.2 Bautin bifurcation

After setting the first Lyapunov coefficient to zero, evaluating the second Lyapunov coefficient is essential for the Bautin bifurcation. This type of bifurcation presents significant challenges to resolve. It is attributed to a family of stable and unstable limit cycles coexisting, with one nested within the other, colliding, and eventually disappearing through a saddle-node bifurcation. Control over this process is crucial as it substantially influences both the stability of the equilibrium and the trajectory of the resulting limit cycle.

In this section, we will briefly explain the Bautin bifurcation. The next section will focus on controlling such bifurcation. The relevant theorem and its proof, provided by [28], are as follows.

Theorem 2.1.2 *Consider the planar nonlinear system given by (2.4) depending on the parameter $\mu \in \mathbb{R}^2$ with the equilibrium at the origin and a pair of purely imaginary eigenvalues $\lambda(0) = \pm i\omega_0$, $\omega_0 > 0$.*

Let $l_1(0) = 0$. If the system satisfies the following conditions:

(b.i) $l_2(0) \neq 0$ where $l_2(\mu)$ is the second Lyapunov coefficient,

(b.ii) The map $\mu \mapsto (\eta(\mu), l_1(\mu))$ is regular at $\mu = 0$,

then, by a linear and nonlinear complex coordinate shift, a linear time scale, and a nonlinear time reparametrisation, the system can be transformed into the complex form

$$\dot{u} = (\kappa_1 + i)u + \kappa_2 |u|^2 u + s|u|^4 u + O(\|u\|^6)\tag{2.26}$$

where $s = \text{sign}[l_2(0)] = \pm 1$.

Proof 2.1.2 The steps are quite similar to the ones in Proof 2.1.1. All g_{kl} related to the second Lyapunov coefficient are calculated in a similar way such that

$$g_{40}(0) = \langle p, D_i(q, q, q, q) \rangle, \quad k = 4, \quad l = 0, \quad i = 1, 2,$$

$$g_{31}(0) = \langle p, D_i(q, q, q, \bar{q}) \rangle, \quad k = 3, \quad l = 1, \quad i = 1, 2,$$

$$g_{22}(0) = \langle p, D_i(q, q, \bar{q}, \bar{q}) \rangle, \quad k = 2, \quad l = 2, \quad i = 1, 2,$$

$$g_{13}(0) = \langle p, D_i(q, \bar{q}, \bar{q}, \bar{q}) \rangle, \quad k = 1, \quad l = 3, \quad i = 1, 2$$

where

$$D_i(x, y, z, t) = \sum_{j,k,l,m=1}^2 \frac{\partial^4 F_i(\xi)}{\partial \xi_j \partial \xi_k \partial \xi_l \partial \xi_m} \Big|_{\xi=0} x_j y_k z_l t_m, \quad i = 1, 2, \quad (2.27)$$

and

$$g_{32}(0) = \langle p, E_i(q, q, q, \bar{q}, \bar{q}) \rangle, \quad k = 3, \quad l = 2, \quad i = 1, 2$$

where

$$E_i(x, y, z, t, r) = \sum_{j,k,l,m,n=1}^2 \frac{\partial^5 F_i(\xi)}{\partial \xi_j \partial \xi_k \partial \xi_l \partial \xi_m \partial \xi_n} \Big|_{\xi=0} x_j y_k z_l t_m r_n, \quad i = 1, 2. \quad (2.28)$$

$D = (D_1, D_2)^T$ and $E = (E_1, E_2)^T$ are also symmetric multilinear vector-valued functions of $x, y, z, t, r \in \mathbb{R}^2$.

Further, we will expand the system up to the sixth-order terms as

$$\dot{z} = \lambda z + \sum_{2 \leq k+l \leq 5} \frac{1}{k!l!} g_{kl}(\mu) z^k \bar{z}^l + O(\|z\|^6) \quad (2.29)$$

and try to eliminate the fourth and fifth-order terms. Let us introduce an integrated nonlinear complex coordinate depending on an invertible parameter w by

$$z = w + \sum_{2 \leq k+l \leq 5} \frac{1}{k!l!} h_{kl}(\mu) w^k \bar{w}^l. \quad (2.30)$$

By substituting the last two equations above in \dot{w} , the derivative of the inverse of z , and then by setting each h_{kl} , all the fourth-order terms and all but one of the fifth-order terms are eliminated, and it yields the following equation

$$\dot{w} = \lambda(\mu)w + c_1(\mu)|w|^2 w + c_2(\mu)|w|^4 w + O(\|w\|^6) \quad (2.31)$$

where c_1 and c_2 are the complex coefficients of the resonant cubic and fifth-order terms, respectively.

By the linear time variable $\tau = \omega(\mu)t$, the equation (2.31) can be expressed as

$$\frac{dw}{d\tau} = (n(\mu) + i)w + d_1(\mu)|w|^2w + d_2(\mu)|w|^4w + O(\|w\|^6) \quad (2.32)$$

where

$$n(\mu) = \frac{\eta(\mu)}{\omega(\mu)}, \quad d_1(\mu) = \frac{c_1(\mu)}{\omega(\mu)}, \quad d_2(\mu) = \frac{c_2(\mu)}{\omega(\mu)}.$$

Here, the coefficients $d_{1,2}(\mu)$ are complex.

Considering the nonlinear time variable $d\tau = (1 + e_1(\mu)|w|^2 + e_2(\mu)|w|^4)d\theta$ where

$$e_1(\mu) = -\text{Im}[d_1(\mu)], \quad e_2(\mu) = -\text{Im}[d_2(\mu)] + (\text{Im}[d_1(\mu)])^2,$$

the equation (2.32) transforms into the following equation

$$\frac{dw}{d\theta} = (n(\mu) + i)w + l_1(\mu)|w|^2w + l_2(\mu)|w|^4w + O(\|w\|^6) \quad (2.33)$$

where

$$l_1(\mu) = \text{Re}[d_1(\mu)] - n(\mu)d_1(\mu) = \frac{\text{Re}[c_1(\mu)]}{\omega(\mu)} - \eta(\mu) \frac{\text{Im}[c_1(\mu)]}{(\omega(\mu))^2}$$

is the first Lyapunov coefficient, as in (2.22) at $\mu = 0$, and

$$l_2(\mu) = \text{Re}[d_2(\mu)] - \text{Re}[d_1(\mu)]\text{Im}[d_1(\mu)] + n(\mu) \left((\text{Im}[d_1(\mu)])^2 - \text{Im}[d_2(\mu)] \right)$$

is the second Lyapunov coefficient. We note that both the coefficients $l_{1,2}(\mu)$ and $e_{1,2}(\mu)$ are real. At $\mu = 0$, we get

$$l_2(0) = \text{Re} \left[\frac{c_2(0)}{\omega_0} \right] \quad (2.34)$$

where the first Lyapunov coefficient vanishes.

The second Lyapunov coefficient at the origin is then given by

$$\begin{aligned}
12l_2(0,0) = & \frac{1}{\omega_0} \operatorname{Re}[g_{32}] + \\
& \frac{1}{\omega_0^2} \operatorname{Im} \left[g_{20}\bar{g}_{31} - g_{11}(4g_{31} + 3\bar{g}_{22}) - \frac{1}{3}g_{02}(g_{40} + \bar{g}_{13}) - g_{30}g_{12} \right] + \\
& \frac{1}{\omega_0^3} \left\{ \operatorname{Re} \left[g_{20} \left(\bar{g}_{11}(3g_{12} - \bar{g}_{30}) + g_{02} \left(\bar{g}_{12} - \frac{1}{3}g_{30} \right) + \frac{1}{3}\bar{g}_{02}g_{03} \right) + \right. \right. \\
& \quad \left. \left. g_{11} \left(\bar{g}_{02} \left(\frac{5}{3}\bar{g}_{30} + 3g_{12} \right) + \frac{1}{3}g_{02}\bar{g}_{03} - 4g_{11}g_{30} \right) \right] + \right. \\
& \quad \left. 3 \operatorname{Im} [g_{20}g_{11}] \operatorname{Im}[g_{21}] \right\} + \\
& \frac{1}{\omega_0^4} \left\{ \operatorname{Im} \left[g_{11}\bar{g}_{02} \left(\bar{g}_{20}^2 - 3\bar{g}_{20}g_{11} - 4g_{11}^2 \right) \right] + \right. \\
& \quad \left. \operatorname{Im} [g_{20}g_{11}] \left(3 \operatorname{Re} [g_{20}g_{11}] - 2|g_{02}|^2 \right) \right\}. \tag{2.35}
\end{aligned}$$

Let us define a map

$$\mu \mapsto \left(\operatorname{Re} [\lambda_{1,2}(\mu)], l_1(\mu) \right), \quad \operatorname{Re} [\lambda_{1,2}(\mu)] = \eta(\mu), \quad \mu = (\mu_1, \mu_2).$$

Since the following holds

$$\begin{vmatrix} \frac{\partial \eta(\mu_1, \mu_2)}{\partial \mu_1} & \frac{\partial \eta(\mu_1, \mu_2)}{\partial \mu_2} \\ \frac{\partial l_1(\mu_1, \mu_2)}{\partial \mu_1} & \frac{\partial l_1(\mu_1, \mu_2)}{\partial \mu_2} \end{vmatrix} \neq 0,$$

the map is regular at $\mu = 0$, and it satisfies the condition (b.ii). We can write μ as a function of η . Substituting $\eta_1 = n(\mu)$ and $\eta_2 = l_1(\mu)$, the equation (2.33) is then written as follows

$$\frac{dw}{d\theta} = (\eta_1 + i)w + \eta_2|w|^2w + L_2(\eta)|w|^4w + O(\|w\|^6) \tag{2.36}$$

where $L_2(\eta) = l_2(\mu(\eta))$ is not equal to zero at μ .

Using the linear complex coordinate u defined as $w = \sqrt[4]{|L_2(\eta)|}u$ where $L_2(0) = l_2(0) \neq 0$ (b.i), and using the parameters $\kappa_1 = \eta_1$, $\kappa_2 = \eta_1 \sqrt{|L_2(\eta)|}$, we get the final complex form

$$\frac{du}{d\theta} = (\kappa_1 + i)u + \kappa_2|u|^2u + s|u|^4u + O(\|u\|^6) \tag{2.37}$$

where $s = \operatorname{sign} [l_2(0)] = \pm 1$. \square

2.2 Control of Hopf and Bautin Bifurcation

A considerable number of reference articles are available in the literature, discussing control laws for both linear and nonlinear systems. In this study, we will follow the control law proposed by Braga et al. in 2010 [26]. This control law, depending on two bifurcation parameters and four control parameters, is an offer to regulate bifurcation features and generate controllable Hopf and Bautin bifurcation. The relevant theorem is presented below.

Theorem 2.2.1 *Let $H, G : \mathbb{R}^2 \rightarrow \mathbb{R}^2$ be smooth vector fields, and $G(x)U(x, \mu, \beta)$ be a control law where*

$$U(x, \mu, \beta) = \beta_1 \mu_1 + (\beta_2 + \mu_2)(x_1^2 + x_2^2) + \beta_3(x_1^2 + x_2^2)^2, \quad (2.38)$$

$\mu_1, \mu_2 \in \mathbb{R}$ are the bifurcation parameters, and $\beta_1, \beta_2, \beta_3, \text{tr}(dG(0)) \in \mathbb{R}$ are the control parameters. Consider the following planar nonlinear system with the control

$$\dot{x} = H(x) + G(x)U(x, \mu, \beta), \quad x = (x_1, x_2)^T \in \mathbb{R}^2 \quad (2.39)$$

where $H(0) = 0$ and $G(0) = 0$. Here, $dH(0)$ has purely imaginary eigenvalues and $\text{tr}(dG(0)) \neq 0$. Then, there exist β_1, β_2 leading the system to undergo a Hopf bifurcation at $\mu_1 = 0$ provided that $\beta_2 \neq \beta_{2\text{crit}}(\mu_2)$. Besides, there exist $\beta_1, \beta_2, \beta_3$ leading the system to undergo a Bautin bifurcation at $\mu_1 = \mu_2 = 0$ provided that $\beta_2 = \beta_{2\text{crit}}(0)$ and $\beta_3 \neq \beta_{3\text{crit}}$.

We note that $\beta_{2\text{crit}}$ is the critical value of β_2 for which the first Lyapunov coefficient vanishes; and $\beta_{3\text{crit}}$ is the critical value of β_3 for which the second Lyapunov coefficient vanishes.

In other words, there is a unique critical value of $\beta_2 = \beta_{2\text{crit}}$ such that $l_1(0, \mu_2) = 0$ at $\mu_1 = 0$; and there is a unique critical value of $\beta_3 = \beta_{3\text{crit}}$ such that $l_2(0, 0) = 0$ at $\mu_1 = \mu_2 = 0$.

Furthermore, the stability and the direction of the limit cycles emerging near the origin is controllable by selecting $\beta_1 \neq 0, \text{tr}(dG(0)) \neq 0, \beta_2 \neq \beta_{2\text{crit}}$ and $\beta_3 \neq \beta_{3\text{crit}}$.

2.3 Goodwin Model and Modifications

2.3.1 Original Goodwin model

Goodwin model of growth cycle [1], first presented by Richard M. Goodwin in 1967, resembles the classical Lotka-Volterra predator-prey model [2,3]. Both models explore the dynamics of groups. The predator-prey model represents the interaction between predator and prey populations as time progresses. Dynamic equations of the Goodwin model formulate time-dependent potential states of economic activities such as capital, wages, unemployment, and labour.

The Goodwin model [1] comprises two dynamic equations:

$$\begin{aligned}\dot{u}(t) &= \left(\rho v(t) - (\alpha + \varphi) \right) u(t), \\ \dot{v}(t) &= \left(\frac{1 - u(t)}{\zeta} - (\alpha + \gamma) \right) v(t)\end{aligned}\tag{2.40}$$

where $u(t)$ is the share of labour in national income, and $v(t)$ is the proportion of labour force employment. The first equation describing the share equation, incorporates positive constants ρ and φ . The latter, referring to the employment rate, involves the parameters: exogenous growth rate in the labour productivity α , exogenous growth rate in the labour force γ , and the capital-output ratio ζ . The second equation assumes all profits are invested; however, $u(t)$ may exceed the unit value due to disinvestment. Solutions of the system exhibit clockwise closed cycles, each centered at the singular point (\tilde{u}, \tilde{v}) where

$$(\tilde{u}, \tilde{v}) = \left(1 - \zeta(\alpha + \gamma), \frac{\alpha + \varphi}{\rho} \right).$$

\tilde{u} may exceed one for $\alpha + \gamma < 0$ whereas it is inherently less than one for $\alpha + \gamma > 0$. Similarly, \tilde{v} may surpass one. It implies that the singular point (\tilde{u}, \tilde{v}) may extend beyond the unit area, leading to trajectories that partially or entirely exist outside that area. Even if the singular point remains within the unit box, trajectories could extend partially outside its boundaries. As a result, values surpassing one produce impractical outcomes for both the labour share and the employment rate. Several studies have attempted to adapt the Goodwin model to meet this requirement [11–20].

2.3.2 Desai's modified Goodwin model

The modified Goodwin model proposed by Desai et al. [27] is one of the studies satisfying the requirement stated in Section 2.3.1. All trajectories lie inside the unit square in the system's phase portrait. This modified system is defined as follows

$$\begin{aligned}\dot{u} &= \left(\rho(1-v)^{-\delta} - (\alpha + \varphi) \right) u, \\ \dot{v} &= \left(\lambda \ln(\tilde{u} - u) - \lambda \ln(1 - \tilde{u}) - (\alpha + \gamma) \right) v\end{aligned}\tag{2.41}$$

where $\delta > 0$, $\lambda > 0$, $\rho < \alpha + \varphi$, $u < \tilde{u} < 1$, $\frac{\tilde{u}}{1 - \tilde{u}} > 1$ and $\alpha + \gamma < \lambda \ln \frac{\tilde{u}}{1 - \tilde{u}}$. The parameter \tilde{u} refers to the maximum share of labour that capitalists would tolerate, and hence the constraint $\frac{\tilde{u}}{1 - \tilde{u}} > 1$ implies that \tilde{u} is greater than 50%. This modified approach enables the system to experience controllable Hopf or Bautin bifurcation, providing valuable insights into the controllability of the system's dynamics and its response to parameter variations.

By setting δ to be 1 and defining new parameters $k = \frac{\alpha + \varphi}{\rho}$ and $m = \frac{\alpha + \gamma}{\lambda}$, the model given by (2.41) reduces to the following system:

$$\begin{aligned}\dot{u} &= \rho \left((1-v)^{-1} - k \right) u, \\ \dot{v} &= \lambda \left(\ln \frac{\tilde{u} - u}{1 - \tilde{u}} - m \right) v.\end{aligned}\tag{2.42}$$

We assume δ to be 1, thereby simplifying the calculations. It is also possible to conduct a similar analysis for other values of δ .

3. CONTROL OF HOPF AND BAUTIN BIFURCATION IN A MODIFIED GOODWIN MODEL

We have introduced Braga et al.'s control law and the original and Desai et al.'s modified version of the Goodwin model in Chapter 2. In this chapter, we will perform a Hopf and Bautin bifurcation analysis and conduct simulations on the modified Goodwin model [27], employing the control law in [26].

3.1 Equilibrium and Linearisation

We start by determining the equilibrium of the modified nonlinear system (2.42) and linearising it in the neighbourhood of its equilibrium. For $u > 0$ and $v > 0$, the unique equilibrium is localised at

$$(u_0, v_0) = \left(\tilde{u} - e^m(1 - \tilde{u}), 1 - \frac{1}{k} \right)$$

and the substitutions

$$u \rightarrow X_1 - e^m(1 - \tilde{u}) + \tilde{u} \quad \text{and} \quad v \rightarrow X_2 + 1 - \frac{1}{k}$$

transform the equilibrium to the origin. Hence, the modified system (2.42) takes the following form

$$\begin{aligned} \dot{X}_1 &= -\rho k^2 \left(e^m(\tilde{u} - 1) + \tilde{u} + X_1 \right) \frac{X_2}{kX_2 - 1}, \\ \dot{X}_2 &= \lambda \left(1 - \frac{1}{k} + X_2 \right) \left(-m + \ln \frac{e^m(1 - \tilde{u}) - X_1}{1 - \tilde{u}} \right). \end{aligned} \quad (3.1)$$

The Jacobian matrix of (3.1) is

$$J = \begin{pmatrix} -\rho k^2 \frac{X_2}{kX_2 - 1} & \rho k^2 \frac{e^m(\tilde{u} - 1) + \tilde{u} + X_1}{(kX_2 - 1)^2} \\ \frac{\lambda}{k} \frac{kX_2 + k - 1}{e^m(\tilde{u} - 1) + X_1} & \lambda \left(-m + \ln \left(e^m + \frac{X_1}{\tilde{u} - 1} \right) \right) \end{pmatrix}$$

and the corresponding matrix at the origin is

$$A = \begin{pmatrix} 0 & \rho k^2 (e^m(\tilde{u} - 1) + \tilde{u}) \\ \frac{\lambda(k-1)}{ke^m(\tilde{u}-1)} & 0 \end{pmatrix}. \quad (3.2)$$

The matrix A has a pair of complex conjugate eigenvalues:

$$\lambda_{1,2} = \pm i\omega_0$$

where

$$\omega_0 = \sqrt{\frac{\lambda \rho k (k-1) (e^m (\tilde{u}-1) + \tilde{u})}{e^m (1-\tilde{u})}}. \quad (3.3)$$

Given a pair of purely imaginary eigenvalues, the equilibrium is identified as a center displaying neutral stability. The behaviour of the system near this equilibrium manifests as a collection of closed orbits, each with varying amplitudes determined by the system's initial conditions. These initial conditions play a pivotal role in determining the specific closed orbit governing the system's actual dynamic behaviour.

The solution curves and trajectories of the modified Goodwin model defined by the system of equations in (3.1) are plotted for the parameter values $\lambda = 1$, $\rho = 0.05$, $k = 20.02$, $m = 0.002$, $\tilde{u} = 0.9$ with the initial condition $(0.0002002, -0.05005)$ in Figure 3.1a and Figure 3.1b, respectively. All figures in the study are obtained by the NDSolve command of Mathematica, with a specified accuracy and precision goal of 10 digits.

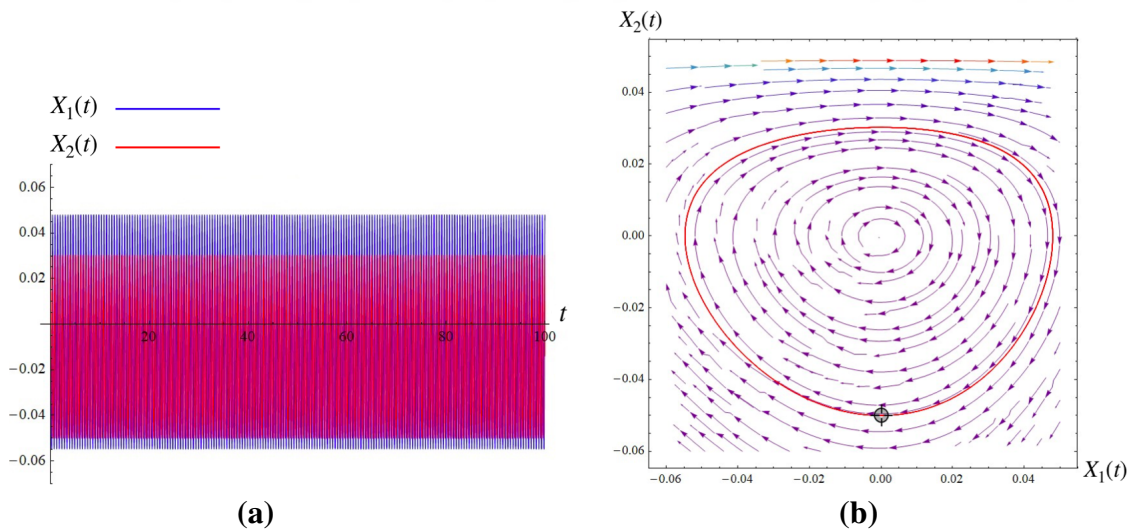


Figure 3.1 : Solution curves and trajectories of the modified Goodwin model for $\lambda = 1$, $\rho = 0.05$, $k = 20.02$, $m = 0.002$, $\tilde{u} = 0.9$ with the initial condition $(0.0002002, -0.05005)$.

3.2 Control of Hopf Bifurcation

This section will focus on generating a controllable Hopf bifurcation in the modified Goodwin model based on Theorem 2.2.1. For the further analysis, we define $H = (H_1, H_2)^T$ as follows

$$H(X) = \begin{pmatrix} H_1(X) \\ H_2(X) \end{pmatrix} = \begin{pmatrix} -\rho k^2 \left(e^m(\tilde{u} - 1) + \tilde{u} + X_1 \right) \frac{X_2}{kX_2 - 1} \\ \lambda \left(1 - \frac{1}{k} + X_2 \right) \left(-m + \ln \frac{e^m(1 - \tilde{u}) - X_1}{1 - \tilde{u}} \right) \end{pmatrix}.$$

Let us incorporate the control input

$$X_i' = H_i(X) + G_i(X)U(X, \mu, \beta), \quad i = 1, 2 \quad (3.4)$$

where U is given by (2.38). For $s \neq 0$, we define the following $G = (G_1, G_2)^T$

$$G(X) = \begin{pmatrix} G_1(X) \\ G_2(X) \end{pmatrix} = \begin{pmatrix} sX_1 \\ sX_2 \end{pmatrix}$$

such that $\text{tr}(dG(0)) \neq 0$. Indeed,

$$M = dG(0) = \begin{pmatrix} s & 0 \\ 0 & s \end{pmatrix}$$

and $\text{tr}(dG(0)) = 2s \neq 0$ for $s \neq 0$. Then, the modified Goodwin model with the control (3.4) is as follows

$$\begin{aligned} X_1' &= -\rho k^2 \left(e^m(\tilde{u} - 1) + \tilde{u} + X_1 \right) \frac{X_2}{kX_2 - 1} + \\ &\quad sX_1 \left(\beta_1 \mu_1 + (\beta_2 + \mu_2)(X_1^2 + X_2^2) + \beta_3(X_1^2 + X_2^2)^2 \right), \\ X_2' &= \lambda \left(1 - \frac{1}{k} + X_2 \right) \left(-m + \ln \frac{e^m(1 - \tilde{u}) - X_1}{1 - \tilde{u}} \right) + \\ &\quad sX_2 \left(\beta_1 \mu_1 + (\beta_2 + \mu_2)(X_1^2 + X_2^2) + \beta_3(X_1^2 + X_2^2)^2 \right), \end{aligned} \quad (3.5)$$

and this final system meets the conditions outlined in Theorem 2.2.1. The Jacobian matrix of (3.5) at the origin

$$A = \begin{pmatrix} \beta_1 \mu_1 s & \rho k^2 \left(e^m(\tilde{u} - 1) + \tilde{u} \right) \\ \frac{\lambda(k-1)}{ke^m(\tilde{u}-1)} & \beta_1 \mu_1 s \end{pmatrix} \quad (3.6)$$

has the following eigenvalues

$$\lambda_{1,2} = \beta_1 \mu_1 s \pm i\omega_0.$$

The derivative below indicates that the transversality condition is satisfied

$$\left. \frac{\partial \operatorname{Re} [\lambda_{1,2}(\mu_1)]}{\partial \mu_1} \right|_{\mu_1=0} = \beta_1 s \neq 0$$

for $\beta_1, s \neq 0$. Considering that the Hopf bifurcation necessitates a pair of purely imaginary eigenvalues and the transversality condition, we fix the bifurcation parameter μ_1 to zero when evaluating the Lyapunov coefficients. We will proceed to calculate the Lyapunov coefficients as presented in [28].

Let $q = (q_1, q_2)^T \in \mathbb{C}^2$ and $p = (p_1, p_2)^T \in \mathbb{C}^2$ be the eigenvectors of A and A^T corresponding to the eigenvalues $\lambda_1 = i\omega_0$ and $\lambda_2 = -i\omega_0$, respectively. We define such vectors as follows

$$q = \begin{pmatrix} \frac{i\omega_0 k e^m (\tilde{u} - 1)}{\lambda(k-1)} \\ 1 \end{pmatrix}, \quad p = \begin{pmatrix} \frac{i\lambda(k-1)}{\omega_0 k e^m (\tilde{u} - 1)} \\ 1 \end{pmatrix}.$$

Here, we have $\langle p, q \rangle = 2 \neq 1$. We normalise p with respect to q by defining

$$q = \begin{pmatrix} \frac{i\omega_0 k e^m (\tilde{u} - 1)}{\lambda(k-1)} \\ 1 \end{pmatrix}, \quad p = \begin{pmatrix} \frac{i\lambda(k-1)}{2\omega_0 k e^m (\tilde{u} - 1)} \\ \frac{-i\lambda(k-1)}{2\omega_0 k e^m (\tilde{u} - 1)} \end{pmatrix}.$$

The first Lyapunov coefficient of the modified Goodwin model with the control is then calculated as

$$l_1(0, \mu_2) = -\frac{2(\beta_2 + \mu_2)s \left(\lambda(1-k) + \rho k^3 e^m (\tilde{u} - 1) (e^m (\tilde{u} - 1) + \tilde{u}) \right)}{\lambda \omega_0 (k-1)} \quad (3.7)$$

where $\mu_1 = 0$, and

$$g_{20} = \frac{(2i\lambda + \omega_0)\omega_0 k}{2\lambda(k-1)} + \frac{\rho k^2 \left((-i\lambda(k-1) + \omega_0)(\tilde{u} - 1) - i\lambda(k-1)e^{-m}\tilde{u} \right)}{\omega_0(\tilde{u} - 1)},$$

$$g_{11} = \frac{k}{2\omega_0} \left(\frac{\omega_0^3}{\lambda(1-k)} - \frac{2i\lambda \rho k(k-1)(e^m(\tilde{u} - 1) + \tilde{u})}{e^m(\tilde{u} - 1)} \right),$$

$$g_{21} = \frac{1}{2} \left\{ 8(\beta_2 + \mu_2)s + \frac{\omega_0^2 k^2 (-\lambda + 2i\omega_0 + 8(\beta_2 + \mu_2)se^{2m}(\tilde{u} - 1)^2)}{\lambda^2(k-1)^2} - \frac{6i\lambda\rho k^4 (e^m(\tilde{u} - 1) + \tilde{u})}{\omega_0 e^m(\tilde{u} - 1)} + 2\rho k^3 \left(1 + \frac{3i\lambda (e^m(\tilde{u} - 1) + \tilde{u})}{\omega_0 e^m(\tilde{u} - 1)} \right) \right\},$$

$$B_1 = \rho k^2 (x_1 y_2 + x_2 y_1 + 2k(e^m(\tilde{u} - 1) + \tilde{u})x_2 y_2),$$

$$B_2 = \frac{\lambda((1-k)x_1 y_1 + ke^m(\tilde{u} - 1)(x_1 y_2 + x_2 y_1))}{ke^{2m}(\tilde{u} - 1)^2},$$

$$C_1 = 2x_2 \left(\rho k^3 (3k(e^m(\tilde{u} - 1) + \tilde{u})y_1 z_2 + y_2 z_1 + y_2 z_2) + (\beta_2 + \mu_2)s(y_1 z_2 + y_2 z_1) \right) + x_1 (2\rho k^3 y_2 z_2 + 2(\beta_2 + \mu_2)s(3y_1 z_1 + y_2 z_2)),$$

$$C_2 = \frac{2\lambda(k-1)x_1 y_1 z_1}{ke^{3m}(\tilde{u} - 1)^3} - \frac{\lambda(x_1 y_1 z_2 + x_1 y_2 z_1 + x_2 y_1 z_1)}{e^{2m}(\tilde{u} - 1)^2} + 2(\beta_2 + \mu_2)s(x_1 y_1 z_2 + x_1 y_2 z_1 + x_2 y_1 z_1 + 3x_2 y_2 z_2).$$

Clearly, the first Lyapunov coefficient (3.7) vanishes at $\beta_{2 \text{crit}}(\mu_2) = -\mu_2$.

By setting the initial condition (0.0002002, -0.05005) and the parameter values $\lambda = 1$, $\rho = 0.05$, $k = 20.02$, $m = 0.002$, $\tilde{u} = 0.9$, $s = 1$, $\beta_1 = 0.3$, $\beta_2 = 0.1$, $\beta_3 = -0.6$, simulation results for various values of the bifurcation parameter μ_1 are shown in Figure 3.2, Figure 3.3 and Figure 3.4. The characteristic solution curves and the corresponding phase portraits illustrate a focus at $\mu_1 = -0.1$ in Figure 3.2; a weakly attracting focus at $\mu_1 = 0$ in Figure 3.3; a stable limit cycle at $\mu_1 = 0.01$ in Figure 3.4. We observe the presence of an equilibrium encircled by an isolated, unique and stable limit cycle in Figure 3.4d. Figure 3.4b and Figure 3.4f further demonstrate that trajectories originating either inside or outside the cycle converge towards it as $t \rightarrow +\infty$.

The system experiences a supercritical Hopf bifurcation ($l_1 < 0$) in the aforementioned cases. Under suitable parameter values, it is also possible that the system undergoes a subcritical Hopf bifurcation ($l_1 > 0$). We would like to emphasize that since the analysis is local, the focus on the Hopf bifurcation is limited to the neighbourhood of the origin, particularly at the parameter value $\mu_1 = 0$.

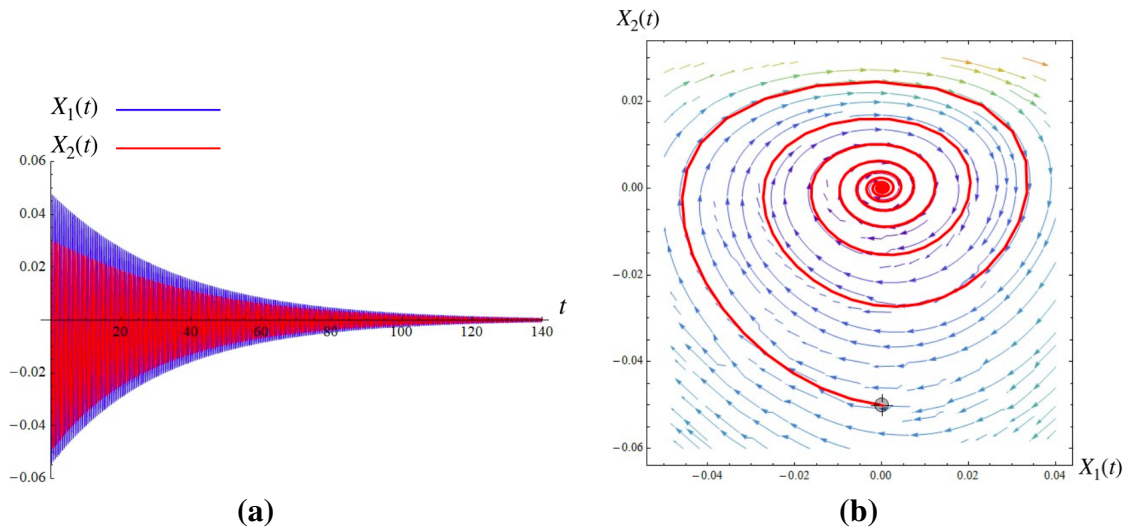


Figure 3.2 : Solution curves and the phase portrait illustrating a focus corresponding to the bifurcation parameter $\mu_1 = -0.1$.

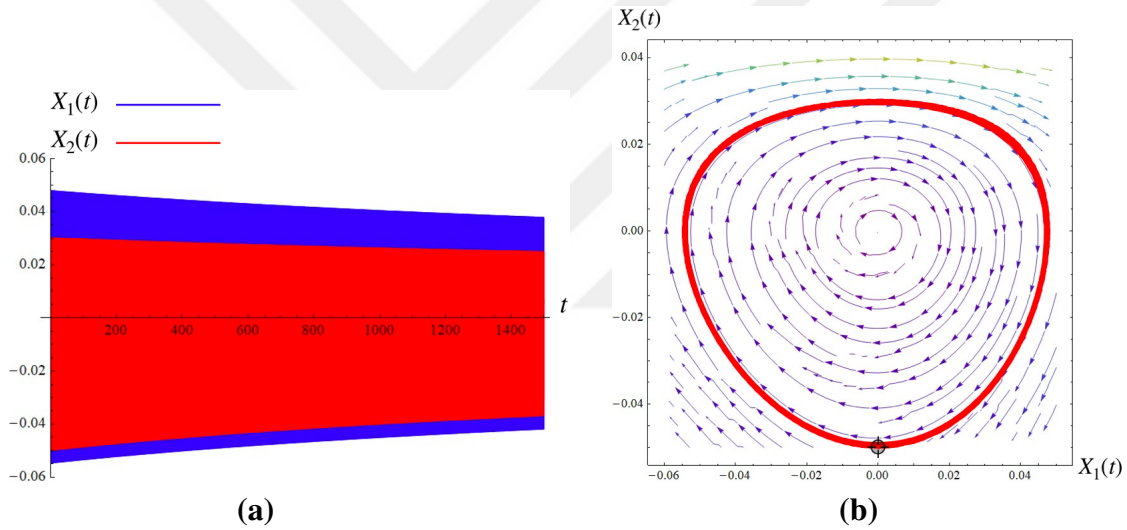


Figure 3.3 : Solution curves and the phase portrait illustrating a weakly attracting focus corresponding to the bifurcation parameter $\mu_1 = 0$.

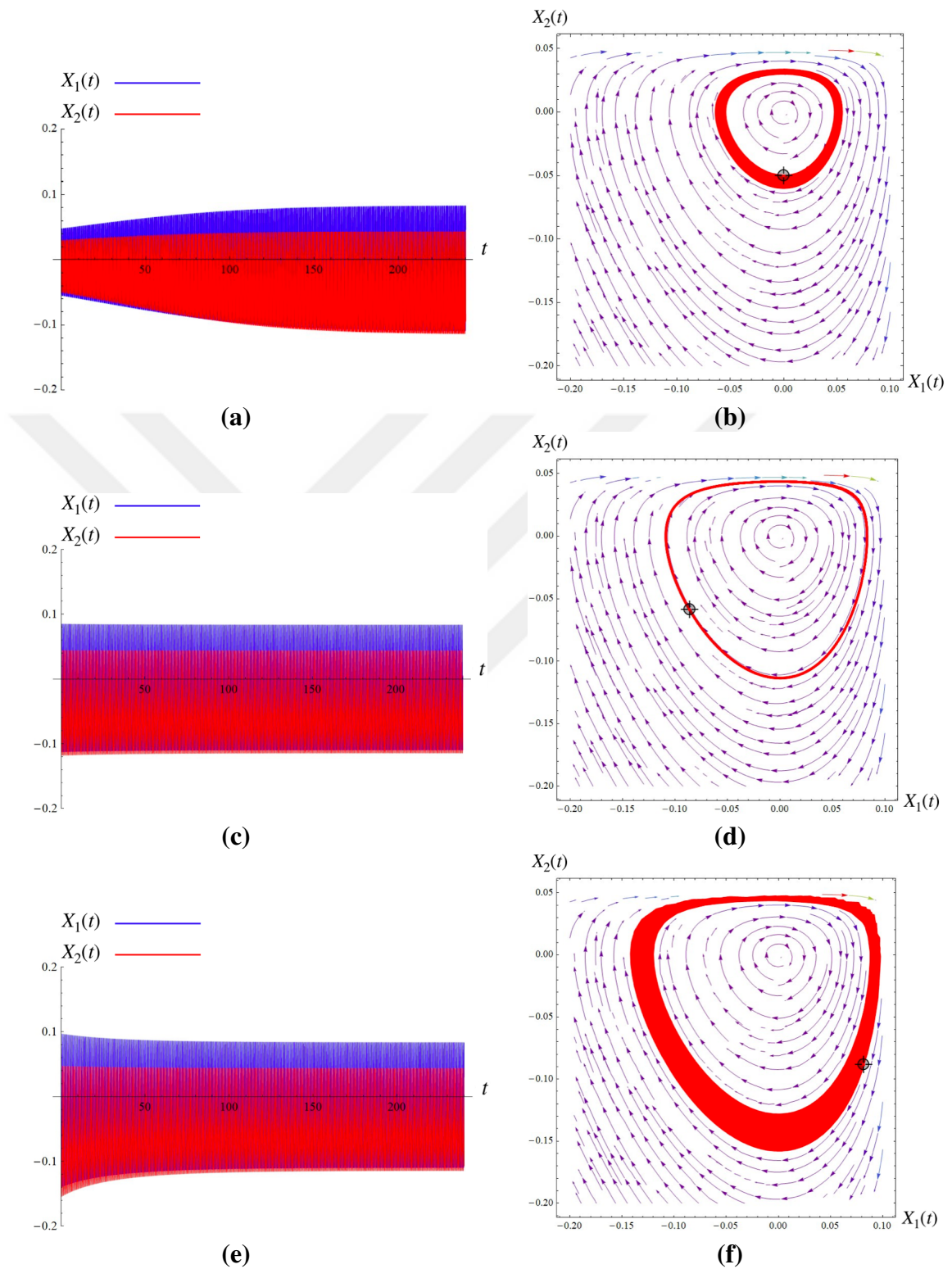


Figure 3.4 : Solution curves and the phase portraits illustrating a stable limit cycle corresponding to the bifurcation parameter $\mu_1 = 0.01$.

3.3 Control of Bautin Bifurcation

The control law in Theorem 2.2.1 has produced effective results for the Hopf bifurcation. Let us confirm it for the Bautin bifurcation. By setting the first Lyapunov coefficient to be zero, the second Lyapunov coefficient of the modified Goodwin model with the control is then calculated as

$$l_2(0,0) = \frac{2\beta_3 s}{\lambda^2 \omega_0 (k-1)^2} \left(3\lambda^2 (k-1)^2 - 2\lambda \rho k^3 (k-1) e^m (\tilde{u}-1) (e^m (\tilde{u}-1) + \tilde{u}) + 3\rho^2 k^6 e^{2m} (\tilde{u}-1)^2 (e^m (\tilde{u}-1) + \tilde{u})^2 \right) \quad (3.8)$$

where $\mu_1 = \mu_2 = 0$, and

$$g_{02}(0) = \frac{(-2i\lambda + \omega_0) \omega_0 k}{2\lambda(k-1)} - \frac{i\rho k^2 (e^m (\lambda(k-1) - i\omega_0) (\tilde{u}-1) + \lambda(k-1)\tilde{u})}{\omega_0 e^m (\tilde{u}-1)},$$

$$g_{30}(0) = \frac{1}{2} \left\{ 12(\beta_2 + \mu_2)s + \frac{\omega_0^2 k^2 (3\lambda - 2i\omega_0 - 12e^{2m}(\beta_2 + \mu_2)s(\tilde{u}-1)^2)}{\lambda^2 (k-1)^2} - \frac{6i\lambda \rho k^4 (e^m (\tilde{u}-1) + \tilde{u})}{\omega_0 e^m (\tilde{u}-1)} + 6\rho k^3 \left(1 + \frac{i\lambda (e^m (\tilde{u}-1) + \tilde{u})}{\omega_0 e^m (\tilde{u}-1)} \right) \right\},$$

$$g_{12}(0) = \frac{1}{2} \left\{ 4(\beta_2 + \mu_2)s + \frac{\omega_0^2 k^2 (-\lambda - 2i\omega_0 - 4e^{2m}(\beta_2 + \mu_2)s(\tilde{u}-1)^2)}{\lambda^2 (k-1)^2} - \frac{6i\lambda \rho k^4 (e^m (\tilde{u}-1) + \tilde{u})}{\omega_0 e^m (\tilde{u}-1)} + 2\rho k^3 \left(-1 + \frac{3i\lambda (e^m (\tilde{u}-1) + \tilde{u})}{\omega_0 e^m (\tilde{u}-1)} \right) \right\},$$

$$g_{03}(0) = \frac{k^2}{2\lambda^2 \omega_0 (k-1)^2 e^m (\tilde{u}-1)} \left(e^m (6\lambda^2 \rho k (k-1)^2 (-i\lambda(k-1) - \omega_0) + \omega_0^3 (3\lambda + 2i\omega_0)) (\tilde{u}-1) - 6i\lambda^3 \rho k (k-1)^3 \tilde{u} \right),$$

$$g_{40}(0) = \frac{k^3}{\omega_0} \left\{ \frac{(-4i\lambda - 3\omega_0) \omega_0^4}{\lambda^3 (k-1)^3} + 12\rho k \left(\omega_0 - \frac{i\lambda (k-1) (e^m (\tilde{u}-1) + \tilde{u})}{e^m (\tilde{u}-1)} \right) \right\},$$

$$g_{31}(0) = \frac{k^3}{\omega_0} \left\{ \frac{(2i\lambda + 3\omega_0) \omega_0^4}{\lambda^3 (k-1)^3} + 6\rho k \left(\omega_0 - \frac{2i\lambda (k-1) (e^m (\tilde{u}-1) + \tilde{u})}{e^m (\tilde{u}-1)} \right) \right\},$$

$$\begin{aligned}
g_{22}(0) &= -\frac{3\omega_0^4 k^3}{\lambda^3(k-1)^3} - \frac{12i\lambda\rho k^4(k-1)(e^m(\tilde{u}-1) + \tilde{u})}{\omega_0 e^m(\tilde{u}-1)}, \\
g_{13}(0) &= \frac{k^3}{\omega_0} \left\{ \frac{(-2i\lambda + 3\omega_0)\omega_0^4}{\lambda^3(k-1)^3} - 12i\rho k \left(-\frac{i\omega_0}{2} + \lambda(k-1) \left(1 + \frac{\tilde{u}}{e^m(\tilde{u}-1)} \right) \right) \right\}, \\
g_{32}(0) &= 3 \left\{ 8\beta_3 s \left(3 + \frac{2\omega_0^2 k^2 e^{2m}(\tilde{u}-1)^2}{\lambda^2(k-1)^2} + \frac{3\omega_0^4 k^4 e^{4m}(\tilde{u}-1)^4}{\lambda^4(k-1)^4} \right) + \right. \\
&\quad \left. \frac{k^4}{\lambda^4 \omega_0 (k-1)^4 e^m(\tilde{u}-1)} \left((-20i\lambda^5 \rho k(k-1)^5 + 4\lambda^4 \rho \omega_0 k(k-1)^4 - \right. \right. \\
&\quad \left. \left. (\lambda \omega_0^4 + 4i\omega_0^5) \omega_0 \right) e^m(\tilde{u}-1) - 20i\lambda^5 \rho k(k-1)^5 \tilde{u} \right) \right\}, \\
D_1 &= 6\rho k^4 \left\{ x_2 y_2 z_1 t_2 + z_2 \left(x_1 y_2 t_2 + x_2 \left\{ y_1 t_2 + y_2 \left(t_1 + 4k(e^m(\tilde{u}-1) + \tilde{u}) t_2 \right) \right\} \right) \right\}, \\
D_2 &= \frac{2\lambda}{k e^{4m}(\tilde{u}-1)^4} \left(-3(k-1)x_1 y_1 z_1 t_1 + \right. \\
&\quad \left. k e^m(\tilde{u}-1) \left(x_1 y_1 z_2 t_1 + z_1 (x_1 y_1 t_2 + x_1 y_2 t_1 + x_2 y_1 t_1) \right) \right), \\
E_1 &= 24 \left\{ \beta_3 s \left(t_1 r_1 (5x_1 y_1 z_1 + x_1 y_2 z_2 + x_2 y_1 z_2 + x_2 y_2 z_1) + \right. \right. \\
&\quad t_1 r_2 (x_1 y_1 z_2 + x_1 y_2 z_1 + x_2 y_1 z_1 + x_2 y_2 z_2) + \\
&\quad t_2 r_1 (x_1 y_1 z_2 + x_1 y_2 z_1 + x_2 y_1 z_1 + x_2 y_2 z_2) + \\
&\quad \left. t_2 r_2 (x_1 y_1 z_1 + x_1 y_2 z_2 + x_2 y_1 z_2 + x_2 y_2 z_1) \right) + \\
&\quad \rho k^5 \left(x_2 y_2 z_2 t_2 r_1 + \right. \\
&\quad \left. r_2 \left\{ x_2 y_2 z_1 t_2 + z_2 \left(x_1 y_2 t_2 + \right. \right. \right. \\
&\quad \left. \left. \left. x_2 \left\{ y_1 t_2 + y_2 \left(t_1 + 5k(e^m(\tilde{u}-1) + \tilde{u}) t_2 \right) \right\} \right) \right\} \right) \right\},
\end{aligned}$$

$$\begin{aligned}
E_2 = & 24\beta_3 s \left(t_1 r_1 (x_1 y_1 z_2 + x_1 y_2 z_1 + x_2 y_1 z_1 + x_2 y_2 z_2) + \right. \\
& t_1 r_2 (x_1 y_1 z_1 + x_1 y_2 z_2 + x_2 y_1 z_2 + x_2 y_2 z_1) + \\
& t_2 r_1 (x_1 y_1 z_1 + x_1 y_2 z_2 + x_2 y_1 z_2 + x_2 y_2 z_1) + \\
& \left. t_2 r_2 (x_1 y_1 z_2 + x_1 y_2 z_1 + x_2 y_1 z_1 + 5x_2 y_2 z_2) \right) + \\
& \frac{1}{ke^{5m}(\bar{u}-1)^5} \left(24\lambda(k-1)x_1 y_1 z_1 t_1 r_1 - \right. \\
& 6\lambda ke^m(\bar{u}-1) \left(x_1 y_1 z_1 t_1 r_2 + \right. \\
& \left. \left. r_1 (x_1 y_1 z_1 t_2 + x_1 y_1 z_2 t_1 + x_1 y_2 z_1 t_1 + x_2 y_1 z_1 t_1) \right) \right).
\end{aligned}$$

The second Lyapunov coefficient (3.8) vanishes where the critical value of β_3 is zero, thereby proceeding the analysis for $\beta_{3 \text{ crit}} = 0$.

By using the same initial condition as in the case of the Hopf bifurcation and choosing the parameter values $s = 0.05$, $\beta_1 = 1$, $\beta_2 = 0$, $\beta_3 = -1$, results for various values of μ_1 and μ_2 are simulated in the following figures. The solution curves and the phase portraits illustrate a single stable equilibrium without any limit cycle for $\mu_1 = \mu_2 = 0$ in Figure 3.5a and Figure 3.5b; $\mu_1 = 0$, $\mu_2 = -0.2$ in Figure 3.6a and Figure 3.6b; $\mu_1 = -1$, $\mu_2 = 0.2$ in Figure 3.7a and Figure 3.7b; $\mu_1 = -1$, $\mu_2 = 0$ in Figure 3.7c and Figure 3.7d; $\mu_1 = -0.5$, $\mu_2 = -0.5$ in Figure 3.7e and Figure 3.7f.

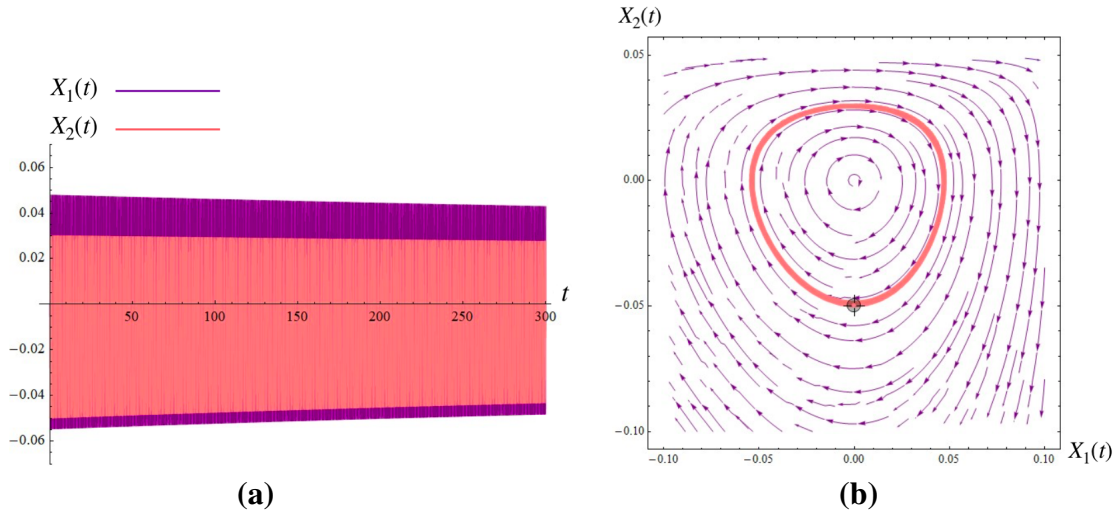


Figure 3.5 : Solution curves and the phase portrait illustrating a sole stable equilibrium without any limit cycle corresponding to the bifurcation parameters $\mu_1 = \mu_2 = 0$.

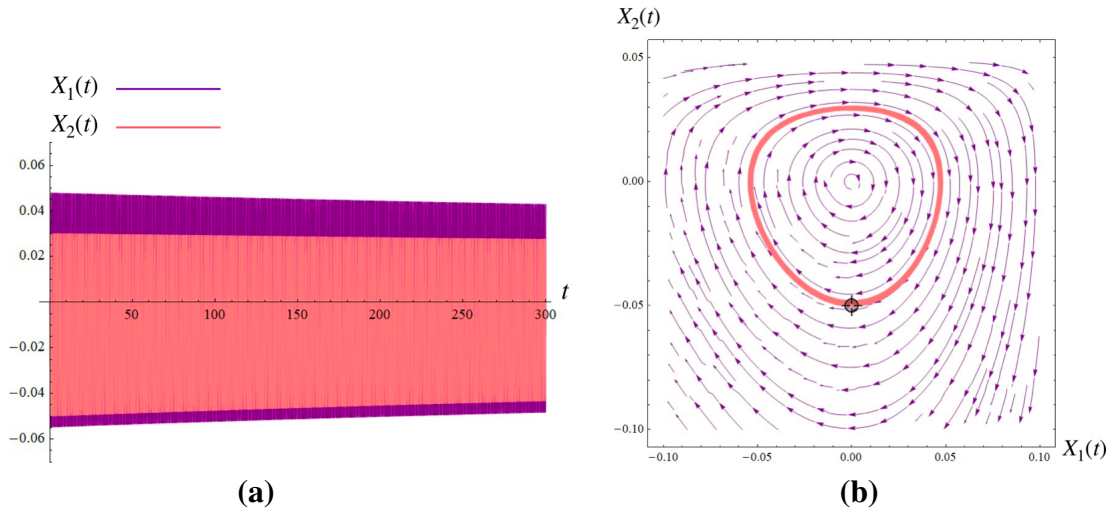


Figure 3.6 : Solution curves and the phase portrait illustrating a sole stable equilibrium without any limit cycle corresponding to the bifurcation parameters $\mu_1 = 0$, $\mu_2 = -0.2$.

A distinct stable limit cycle is observed for $\mu_1 = 0.001$, $\mu_2 = -0.05$ in Figure 3.8, and for $\mu_1 = 0$, $\mu_2 = 0.2$ in Figure 3.9. For $\mu_1 = -0.05$ and $\mu_2 = 0.5$, Figure 3.10 shows the presence of two limit cycles, indicating the presence of an additional unstable cycle within the primary limit cycle. Figure 3.10a portrays the origin as a stable focus, corresponding to the system's behaviour with the initial condition $(0, -1.10^{-9})$, whereas Figure 3.10b is derived for the initial condition $(0, -3.10^{-8})$. Figure 3.10a and Figure 3.10b prove an unstable inner limit cycle of a radius of approximately 10^{-8} between these two behavioural states. Figures 3.10c to 3.10h correspond to initial conditions $(0, -5.10^{-7})$, $(0, -6.10^{-7})$, $(0, -6.10^{-6})$, $(0, -6.10^{-5})$ and $(0, -6.10^{-4})$, respectively. The same initial condition is used in Figure 3.10g and Figure 3.10h. In these figures, trajectories converge to the outer stable limit cycle of a radius of approximately 10^{-7} . Figures 3.10c to 3.10g focus on illustrating this convergence without presenting a comprehensive plot. Whereas Figure 3.10g reveals the limit cycle, Figure 3.10h with the same initial condition as Figure 3.10g exhibits a comprehensive picture.

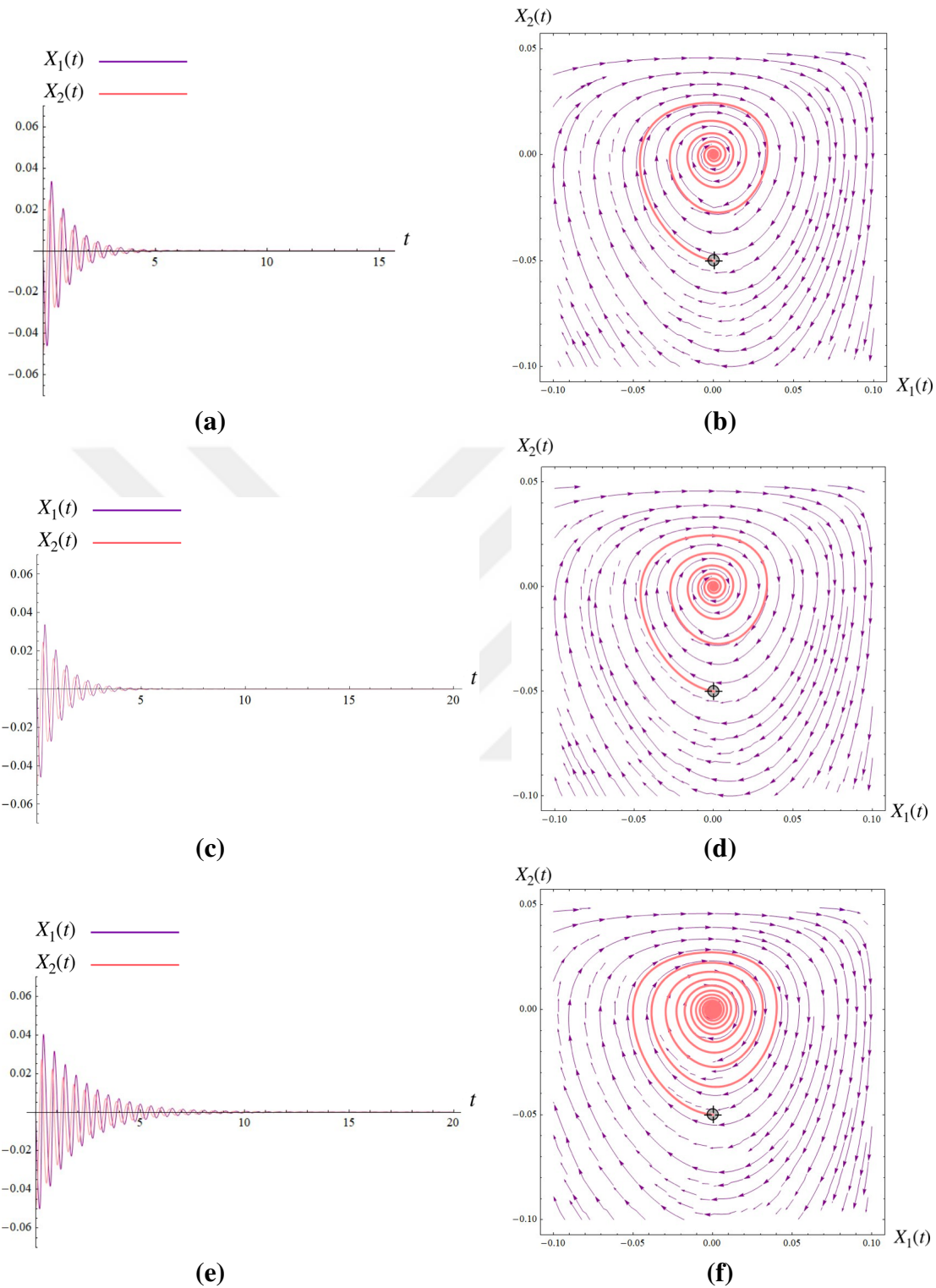


Figure 3.7 : Solution curves and the phase portraits illustrating a sole stable equilibrium without any limit cycle corresponding to the bifurcation parameters $\mu_1 = -1, \mu_2 = 0.2$ in (a) and (b), $\mu_1 = -1, \mu_2 = 0$ in (c) and (d), $\mu_1 = -0.5, \mu_2 = -0.5$ in (e) and (f).

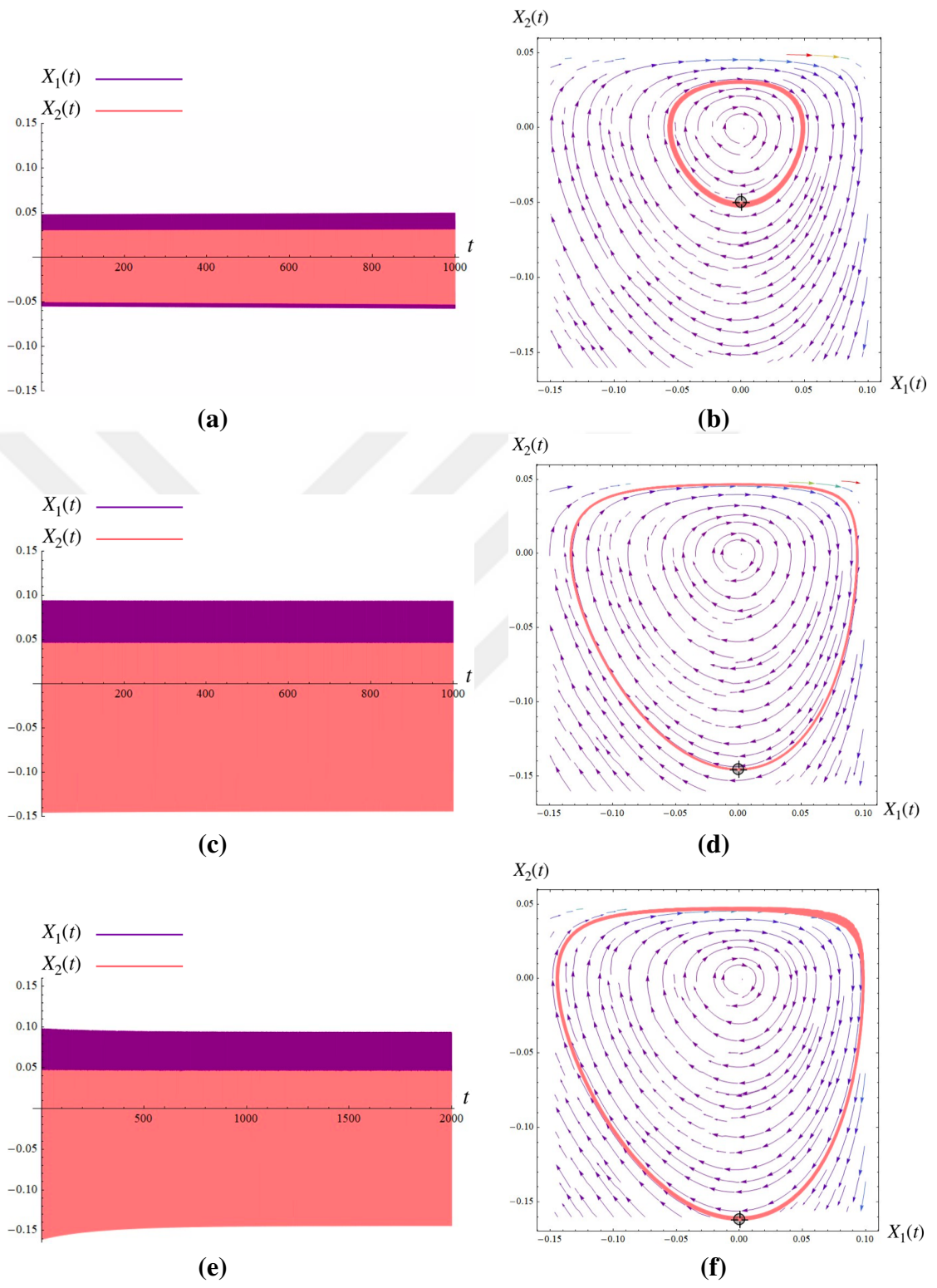


Figure 3.8 : Solution curves and the phase portraits illustrating the presence of a distinct stable limit cycle corresponding to the bifurcation parameters $\mu_1 = 0.0011$, $\mu_2 = -0.05$.

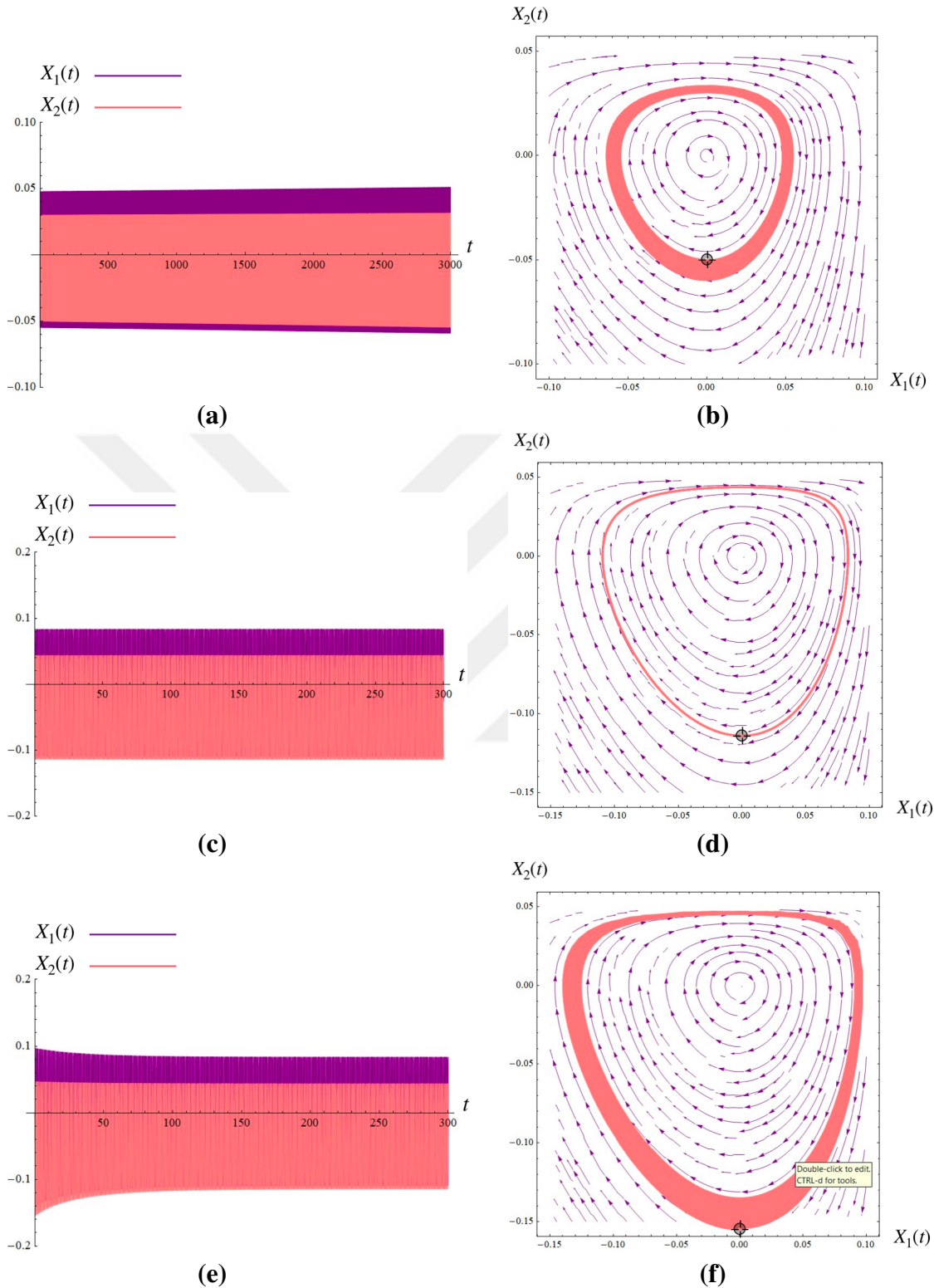


Figure 3.9 : Solution curves and the phase portraits illustrating the presence of a distinct stable limit cycle corresponding to the bifurcation parameters $\mu_1 = 0$, $\mu_2 = 0.2$.

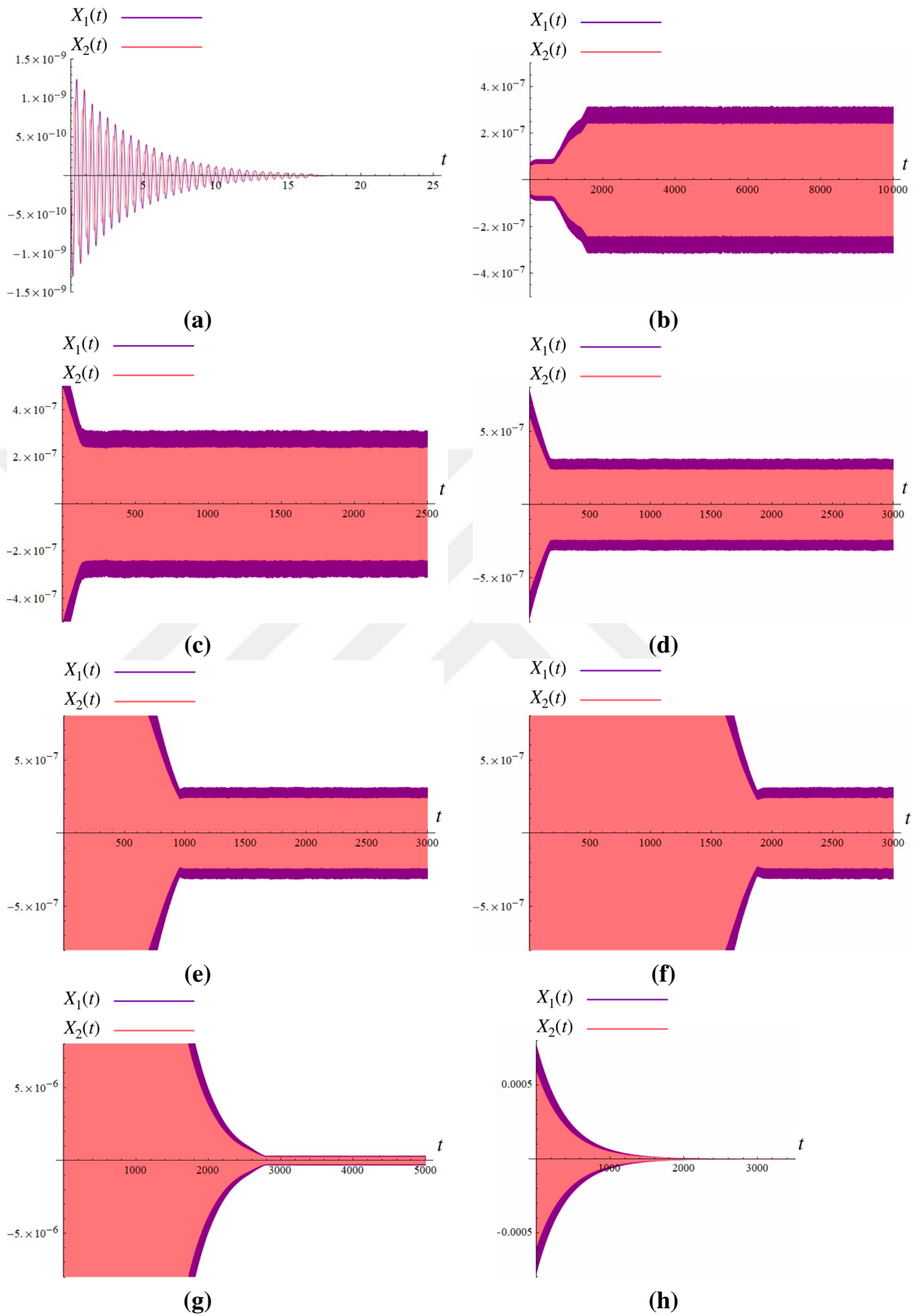


Figure 3.10 : Solution curves illustrating the presence of two limit cycles corresponding to the bifurcation parameters $\mu_1 = -0.05$, $\mu_2 = 0.5$.



4. CONCLUSIONS AND RECOMMENDATIONS

4.1 Conclusions

In this study, we conducted a comprehensive analysis of controlling Hopf bifurcations on Desai et al.'s modified version [27] of the classical Goodwin model [1], which determines the dynamics of class struggle in controlling economic systems. Our investigation involved the systematic manipulation of model parameters to position the economy within the desired regions of the Hopf and Bautin bifurcation diagrams. To achieve this, we developed the necessary steps to identify conditions for producing controllable Hopf and Bautin bifurcation by utilising the control law by Braga et al. [26]. We substantiated our theoretical framework with numerical examples, where we systematically varied control parameters to observe their effects. We observed that minor alterations in parameter values lead to variations in the behaviour of the modified model, resulting in different types of bifurcations.

Through this interdisciplinary analysis, we advanced and expanded the findings regarding the Goodwin model's controllability and focused on bridging theoretical insights with practical applications, thereby offering valuable contributions to policy decisions and strategic interventions to navigate the complexities of economic management.

Given the rich nature of the mathematical foundations, we aim to shed light on the promising applications, particularly within the domains of business cycles and financial and monetary policy. The control parameters introduced in the modified system, as interpreted by Bella to be the fiscal and monetary tools [30], have potential roles in stabilising economies facing undesired cyclical fluctuations.

4.2 Future Suggestions

Future suggestions based on the findings and conclusions of the thesis can be summarised as follows.

1. Exploration of additional factors or variables that may influence the dynamics of class struggle within economic models and their integration into the analysis.
2. Investigation of the broader implications of controllable bifurcations for economic policy-making and stability.
3. Continued research into the theoretical underpinnings of bifurcation theory and its applications in economics, focusing on enhancing our understanding of complex system dynamics.



REFERENCES

- [1] **Goodwin, R.M.**, (1967). A Growth Cycle: Socialism, Capitalism and Economic Growth, 1967, ED. CH Feinstein, Essays in economic dynamics, Springer, pp.165–170.
- [2] **Lotka, A.J.** (1925). *Elements of physical biology*, Williams & Wilkins.
- [3] **Volterra, V.** (1931). Variations and fluctuations of the number of individuals in species living together, p 409–448, *Animal ecology with especial reference to insects*. McGraw-Hill, New York, NY.
- [4] **Desai, M.** (1973). Growth cycles and inflation in a model of the class struggle, *Journal of economic theory*, 6(6), 527–545.
- [5] **Wolfstetter, E.** (1982). Fiscal policy and the classical growth cycle, *Zeitschrift für Nationalökonomie/Journal of Economics*, 42(4), 375–393.
- [6] **van der Ploeg, F.** (1983). Predator-prey and neo-classical models of cyclical growth, *Zeitschrift für Nationalökonomie/Journal of Economics*, 43(3), 235–256.
- [7] **Choi, H.** (1995). Goodwin’s growth cycle and the efficiency wage hypothesis, *Journal of Economic Behavior & Organization*, 27(2), 223–235.
- [8] **Foley, D.K.** (2003). Endogenous technical change with externalities in a classical growth model, *Journal of Economic Behavior & Organization*, 52(2), 167–189.
- [9] **Tavani, D., Zamparelli, L. et al.** (2016). Distributive Conflict, Growth, and the ‘Entrepreneurial State’, **Technical Report**.
- [10] **Atkinson, A.B.** (1969). The timescale of economic models: how long is the long run?, *The Review of Economic Studies*, 36(2), 137–152.
- [11] **Harvie, D., Kelmanson, M.A. and Knapp, D.G.** (2007). A Dynamical Model of Business-Cycle Asymmetries: Extending Goodwin., *Economic Issues*, 12(1).
- [12] **Gaudenzi, M., Madotto, M. and Zanolin, F.** (2013). On the generalizations of the Goodwin model.
- [13] **di Economia Politica, D. and San Francesco, P.** (2001). Growth cycles when workers save.

- [14] **Glombowski, J. and Krüger, M.** (1987). Generalizations of Goodwin's growth cycle model, *Economic Evolution and Structural Adjustment: Proceedings of Invited Sessions on Economic Evolution and Structural Change Held at the 5th International Conference on Mathematical Modelling at the University of California, Berkeley, California, USA July 29–31, 1985*, Springer, pp.260–290.
- [15] **Minsky, H.P.** (1982). Can “it” happen again? A reprise, *Challenge*, 25(3), 5–13.
- [16] **Keen, S.** (1995). Finance and economic breakdown: modeling Minsky's “financial instability hypothesis”, *Journal of Post Keynesian Economics*, 17(4), 607–635.
- [17] **Grasselli, M.R. and Costa Lima, B.** (2012). An analysis of the Keen model for credit expansion, asset price bubbles and financial fragility, *Mathematics and Financial Economics*, 6, 191–210.
- [18] **Grasselli, M.R. and Nguyen Huu, A.** (2015). Inflation and speculation in a dynamic macroeconomic model, *Journal of Risk and Financial Management*, 8(3), 285–310.
- [19] **Tebaldi, C., Colacchio, G. et al.** (2007). Chaotic behavior in a modified goodwin's growth cycle model, *Proceedings of the 25th International Conference of the System Dynamics Society and 50th Anniversary Celebration. System Dynamics Society*.
- [20] **Sportelli, M. and De Cesare, L.** (2022). A Goodwin type cyclical growth model with two-time delays, *Structural Change and Economic Dynamics*, 61, 95–102.
- [21] **Hamzi, B., Kang, W. and Barbot, J.P.** (2004). Analysis and control of Hopf bifurcations, *SIAM journal on control and optimization*, 42(6), 2200–2220.
- [22] **Verduzco, F. and Alvarez, J.** (2004). Hopf bifurcation control for affine systems, *Proceedings of the 2004 American Control Conference*, volume 2, IEEE, pp.1061–1066.
- [23] **Wen, G. and Xu, D.** (2005). Control algorithm for creation of Hopf bifurcations in continuous-time systems of arbitrary dimension, *Physics Letters A*, 337(1-2), 93–100.
- [24] **de Carvalho Braga, D., Mello, L.F., Rocşoreanu, C. and Sterpu, M.** (2011). Controllable Hopf bifurcations of codimensions one and two in linear control systems, *International Journal of Bifurcation and Chaos*, 21(09), 2665–2678.
- [25] **de Carvalho Braga, D., Mello, L.F., Rocşoreanu, C. and Sterpu, M.** (2011). Controllable Hopf bifurcations of codimension 1 and 2 in nonlinear control systems, *Nonlinear Analysis: Theory, Methods & Applications*, 74(9), 3046–3054.

- [26] **de Carvalho Braga, D., Fernando Mello, L., Rocşoreanu, C. and Sterpu, M.** (2010). Control of planar Bautin bifurcation, *Nonlinear Dynamics*, 62, 989–1000.
- [27] **Desai, M., Henry, B., Mosley, A. and Pemberton, M.** (2006). A clarification of the Goodwin model of the growth cycle, *Journal of Economic Dynamics and Control*, 30(12), 2661–2670.
- [28] **Kuznetsov, Y.A., Kuznetsov, I.A. and Kuznetsov, Y.** (1998). *Elements of applied bifurcation theory*, volume 112, Springer.
- [29] **Lynch, S.** (2004). *Dynamical systems with applications using MATLAB*, Springer.
- [30] **Bella, G.** (2013). Multiple cycles and the Bautin bifurcation in the Goodwin model of a class struggle, *Nonlinear Analysis: Modelling and Control*, 18(3), 265–274.





CURRICULUM VITAE

Name Surname : Melike Nur Erdoğan

EDUCATION :

- **B.Sc.** : 2019, Yildiz Technical University, Faculty of Science and Letters, Department of Mathematics

PUBLICATIONS, PRESENTATIONS AND PATENTS ON THE THESIS:

- **Erdoğan M. N.**, Peker-Dobie A., Özemir C. 2024. Control Of Hopf And Bautin Bifurcation In A Modified Goodwin Model Of Growth Cycle. *International Graduate Research Symposium*, March 8–10, 2024 İstanbul, Türkiye.

M. N. ERDOĞAN

CONTROL OF HOPF AND BAUTIN BIFURCATION IN
A MODIFIED GOODWIN MODEL OF GROWTH CYCLE

2024